SIAM J. Applied Dynamical Systems
Vol. 10, No. 4, pp. 1272–1306

Periodically Forced Hopf Bifurcation*

Yanyan Zhang† and Martin Golubitsky‡

Abstract. We study a periodically forced system of ODEs near a point of Hopf bifurcation, where the forcing is pure harmonic, has small amplitude ε, and has forcing frequency ω_F that is near the Hopf frequency ω_H. In this system we vary the forcing frequency and determine all small amplitude periodic solutions to the forced system that have frequency ω_F. In other words, we determine how the number of $\frac{2\pi}{\omega_F}$-periodic solutions to the forced system changes with ω_F. This problem is complicated because of the existence of three small parameters: the amplitude of the forcing ε, the deviation of the bifurcation parameter from the point of Hopf bifurcation λ, and the relative deviation of the forcing frequency from the Hopf frequency $\omega = \frac{\omega_F - \omega_H}{\omega_F}$. Our results are presented in terms of bifurcation diagrams of amplitude of periodic solution versus ω for fixed ε and λ. We assume that the unforced system has a supercritical Hopf bifurcation at $\lambda = 0$ and that the coefficient of the cubic term of the Hopf bifurcation normal form is $\gamma_R + i\gamma_I$. We find that the qualitative form of the bifurcation diagrams depends on $\gamma = \gamma_I/\gamma_R$. For example, if $\lambda < 0$ (so that the equilibrium is stable and there are no small amplitude periodic solutions in the unforced system), then multiplicity of periodic solutions of the forced system occurs in the bifurcation diagrams precisely when $|\gamma| > \sqrt{3}$.

Key words. periodic solutions, Hopf bifurcation, periodic forcing

AMS subject classifications. 34C25, 34C23, 37G15

DOI. 10.1137/10078637X

1. Introduction.

We study a periodically forced system of ODEs near a point of Hopf bifurcation, where the forcing is pure harmonic with small amplitude ε and frequency ω_F. We assume that ω_F is close to the Hopf frequency ω_H. We determine the number of all small amplitude periodic solutions of the forced system that have frequency ω_F as ω_F is varied. In other words, we examine the influence of the forcing frequency ω_F on the number of periodic solutions to the forced system with frequency ω_F. This problem is complicated because of the existence of three small parameters: the amplitude of the forcing ε, the deviation of the bifurcation parameter from the point of Hopf bifurcation λ, and the relative deviation of the forcing frequency from the Hopf frequency $\omega = \frac{\omega_F - \omega_H}{\omega_F}$.

The Introduction is divided into five parts: background on forced systems near Hopf bifurcation, our main result, the methods we use, some remarks about stability of solutions, and an overview of the structure of the paper.

*Received by the editors February 18, 2010; accepted for publication (in revised form) by T. Kaper July 20, 2011; published electronically October 27, 2011. This research was supported in part by NSF grants DMS-0604429, DMS-0931642, and DMS-1008412, and by ARP grant 003652-0009-2006.
http://www.siam.org/journals/siads/10-4/78637.html
†Department of Mathematics, The Ohio State University, Columbus, OH 43210-1174. Current address: CGGVeritas, 10300 Town Park Dr., Houston, TX 77072 (yanyanzhang101@gmail.com).
‡Mathematical Biosciences Institute, The Ohio State University, 1735 Neil Avenue, Columbus, OH 43210 (mg@mbi.osu.edu).

Background. The problem of periodically forced Hopf bifurcation has been studied by many authors [1, 2, 5, 7, 12, 14, 16, 17]. Before describing our results in detail, we describe some of this previous work. Bogoliubov and Mitropolsky [2] give numerous examples of periodically forced systems whose approximate solutions are obtained via multiple methods such as perturbation and spectral methods. However, all systems studied in [2] were assumed to have specific forms in the equations (such as the van der Pol equation) and specific forms in the forcing. Namachchivaya and Ariaratnam [16] considered stability and bifurcation of solutions in the case of subharmonic resonance, that is, $\omega_F = 2\omega_H$. Specifically, they applied the method of averaging to study a two-dimensional autonomous system coupled with simple harmonic forcing. The papers [1, 12, 14, 17] studied harmonic resonance where $\omega_F \approx \omega_H$. Periodic solutions were obtained by a perturbation method by Rosenblat and Cohen [17] and Kath [14], the method of alternative problems by Bajaj [1], and the idea of second-order integral averaging by Gross [12]. Bifurcation diagrams were also considered by these authors. However, [1, 12, 14, 17] worked only on systems with specific forms. As a consequence, their results cannot be applied to general systems directly.

Gambaudo [7] and Elphick, Iooss, and Tirapegui [5] studied dynamics of the forced system without assuming specific forms of the ODEs or the forcing. Gambaudo [7] considered a periodically forced two-dimensional system that is near a Hopf bifurcation point. He took advantage of the weakly nonlinear coordinate changes of Iooss [13] and the Poincaré map to transform the forced system to a normal form, and then determined the dynamics and bifurcations by analyzing the normal form. It is worth remarking that the dynamics and bifurcation diagrams shown in [7] were given in the parameter space whose coordinates are functions of the forcing amplitude ε, the Hopf bifurcation parameter λ in the unforced system, and the frequency deviation ω. In other words, Gambaudo mixed up parameters ε, λ, and ω. Moreover, he did not consider ω as the distinguishing parameter in his study. Elphick, Iooss, and Tirapegui [5] used center manifold theory and Fourier transformations to derive a general amplitude equation for periodic solutions of the system periodically forced near a point of Hopf bifurcation. They [5] claimed but did not prove that the higher-order terms of the amplitude equation do not affect the dynamics of the forced system. In [8], Glendinning and Proctor used a normal form to derive bifurcations. But, as for Gambaudo [7], they did not examine the effect of small changes of ω on the number of periodic solutions.

In the studies mentioned above, these researchers did not investigate the problem of finding all possible bifurcation diagrams of amplitude of periodic solutions of the system versus ω. However, this problem has interested researchers in recent years. For example, Eguíluz et al. [4] studied the effect of ω on periodic responses in the hearing system. But the normal form they used is not generic: they assumed that the cubic term of the normal form has a real coefficient. Montgomery, Silber, and Solla [15] used a generic normal form to study the influence of ω on hearing. They found multiplicity of periodic responses numerically, but they did not determine all possible bifurcation diagrams. In this paper, we both prove the validity of a truncated normal form and classify all bifurcation diagrams of amplitude of periodic solutions versus ω for fixed λ and ε.

Results. In this paper we obtain generic results about periodically forced autonomous systems near a point of Hopf bifurcation. Specifically, we consider the system

$$\dot{x} = F(x, G(t), \lambda), \tag{1.1}$$

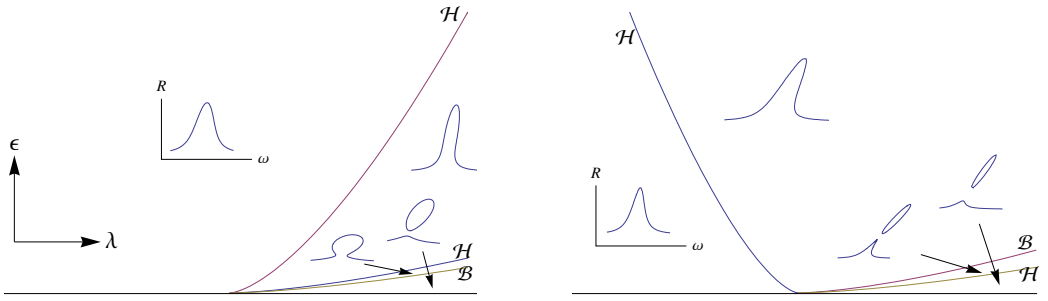

(a) $0 < \gamma < \sqrt{3}$. (b) $\gamma > \sqrt{3}$.

Figure 1. *Bifurcation diagrams of R = amplitude of periodic solution squared versus $\omega \sim 0$ for fixed $\varepsilon \geq 0$ and $\lambda \sim 0$.*

where $x \in \mathbf{R}^n$, $F : \mathbf{R}^n \times \mathbf{R} \times \mathbf{R} \to \mathbf{R}^n$, $\lambda \in \mathbf{R}$, and $G(t) = \mathrm{Re}(ye^{i\omega_F t})$ for $y \in \mathbf{C}$ and $|y| = \varepsilon \ll 1$. We assume that there is an equilibrium of the unforced equation, (1.1) with $G(t) = 0$, at 0 for all λ; that is,

$$F(0, 0, \lambda) = 0. \tag{1.2}$$

We also assume that the unforced equation has a supercritical Hopf bifurcation at $\lambda = 0$. In particular, the Jacobian $(d_x F)_{0,0}$ has simple pure imaginary eigenvalues $\pm\omega_H i$. We assume that the forcing frequency ω_F is near the Hopf frequency ω_H.

Remark 1.1. Note that there is no restriction on the form of F. So F may contain terms such as G^2 that have frequency $2\omega_F$. Hence $G(t)$ may contribute terms in F whose frequency is an arbitrary multiple of ω_F.

We find periodic solutions to the forced system (1.1) that have the same frequency ω_F as the forcing, and we classify the bifurcation diagrams that plot these solutions as ω_F is varied. An important feature of our result is that the bifurcation diagrams that appear depend qualitatively on a constant γ that can be computed directly from the unforced system. More precisely, denote the cubic coefficient in the normal form of the Hopf bifurcation associated with the unforced system by $\gamma_R + i\gamma_I$. Then

$$\gamma = \frac{\gamma_I}{\gamma_R}. \tag{1.3}$$

The qualitative forms of the bifurcation diagrams are given in Figure 1. In these diagrams the amplitude of the forcing ε and the Hopf bifurcation parameter λ are held fixed, as is the constant γ. We see that there are several transitions in the bifurcation diagrams as ε and λ themselves are varied. Moreover, the qualitative features of the transitions depend on whether or not $|\gamma| > \sqrt{3}$. This observation (though not the complete classification of bifurcation diagrams) was noted previously in [9] for periodic forcing of the Hopf normal form system by additive pure harmonic forcing. In particular, when $\lambda < 0$ (that is, when the equilibrium in the unforced system is stable), multiplicity of responses occurs only when $\gamma > \sqrt{3}$. The five different bifurcation diagrams are shown in Figure 2.

We make three comments about the results summarized in Figure 1. First, when $\lambda < 0$, there is a unique equilibrium and no periodic solutions in the unforced system. Thus, it follows

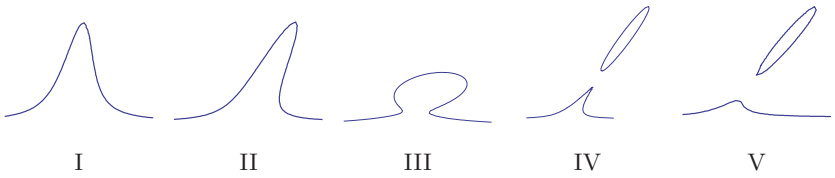

Figure 2. *The types of bifurcation diagrams of amplitude versus ω.*

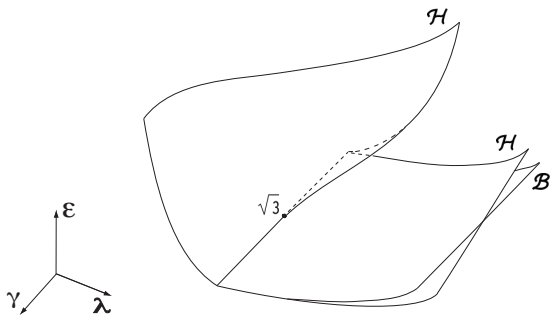

Figure 3. *Picture of the surfaces where hysteresis $\mathcal{H}$ and bifurcation $\mathcal{B}$ occur in $(\lambda, \varepsilon, \gamma)$ parameter space with $\gamma \sim \sqrt{3}$.*

from standard theory that for negative λ and ε sufficiently small (depending on λ) there is a unique periodic solution to the forced system with frequency ω_F. However, Figure 1 shows more. If $0 < \gamma < \sqrt{3}$, then for any small negative λ and small positive ε there is a unique solution to the normal form (1.8) of the forced system when $\omega \sim 0$. On the other hand, when $\gamma > \sqrt{3}$ and $\lambda < 0$, (1.8) may have multiple solutions near $\omega = 0$ for a range of small ε.

Second, note that for fixed $\lambda > 0$ and all ε small enough we can find three solutions for some values of $\omega \sim 0$. The extra solutions derive from the periodic solutions associated with the supercritical Hopf bifurcation in the unforced system.

Finally we comment about the transition varieties themselves. Bifurcation points exist only when λ is positive. In addition, when γ moves across $\sqrt{3}$, one of the hysteresis curves switches from one side of the (λ, ε) parameter plane to the other. From Figures 1(a) and 1(b), it seems as though when γ increases past $\sqrt{3}$, the slope of the tangent line of one of the hysteresis curves *jumps* from positive to negative. However, in Figure 3, we see that the tangency of the hysteresis curve changes smoothly for $\gamma \sim \sqrt{3}$ if we look at the two-dimensional hysteresis and bifurcation sets in three-dimensional $(\lambda, \varepsilon, \gamma)$ space.

Methods. We adapt the standard proof of the Hopf bifurcation theorem using Liapunov–Schmidt reduction on loop space and $\mathbf{S}^1$ symmetry to the case of forced systems. We then use $\mathbf{S}^1$-equivariant singularity theory to obtain a cubic equation in R (a parameter that is an invertible function of the square of the amplitude of periodic solutions of the forced equation), whose zeros correspond to the desired periodic solutions. The coefficients of this cubic equation depend on $\varepsilon, \lambda, \gamma$. See (1.8) below. Figure 1 is obtained by qualitatively graphing the solutions of this cubic equation. We begin by indicating how Liapunov–Schmidt reduction on loop space

can be adapted to the forced equation in such a way that $\mathbf{S}^1$ symmetry is preserved.

Introduce a new time $s = \omega_F t$ so that the forcing has frequency 1; then the system has the form

$$\frac{dx}{ds} = \frac{1}{\omega_F} F(x, \tilde{G}(s), \lambda),$$

where $\tilde{G}(s) = \mathrm{Re}(ye^{is})$. To obtain the number of 2π-periodic solutions to this system with ω_F varying near the Hopf frequency ω_H, we set $\omega = \frac{\omega_F - \omega_H}{\omega_F}$ and investigate the effect of ω on the number of 2π-periodic solutions. Thus, we look at the system

$$\frac{dx}{ds} = \frac{1-\omega}{\omega_H} F(x, \tilde{G}, \lambda) \equiv \tilde{F}(x, \tilde{G}, \omega, \lambda). \tag{1.4}$$

For convenience, we drop the tildes over F and G in (1.4). Then we have

$$\frac{dx}{ds} = F(x, G(s), \omega, \lambda), \tag{1.5}$$

where $G(s) = \mathrm{Re}(ye^{is})$ has small amplitude ε, and λ and ω are small.

Let $A(\omega, \lambda) = (d_x F)_{0,0,\omega,\lambda}$. The occurrence of a generic Hopf bifurcation at 0 gives rise to simple eigenvalues $\sigma(\omega, \lambda) \pm i\kappa(\omega, \lambda)$ for $A(\omega, \lambda)$, and all other eigenvalues are off the imaginary axis as $\lambda \sim 0$ (see Appendix A for conditions for occurrence of a Hopf bifurcation). Moreover, by considering (1.4), we have

$$\begin{array}{ll} \text{(a)} & \kappa(\omega, 0) = 1 - \omega, \\ \text{(b)} & \sigma_\lambda(0) \neq 0. \end{array} \tag{1.6}$$

By using Liapunov–Schmidt reduction (Golubitsky and Schaeffer [10]) and equivariant singularity theory (see Damon [3], Golubitsky, Stewart, and Schaeffer [11], and Furter, Sitta, and Stewart [6]), we show that generically for fixed small y and λ the small 2π-periodic solutions to (1.5) are in one-to-one correspondence with the zeros of a complex-valued function that can be transformed by invertible coordinate changes to

$$\Psi(z, y, \omega, \lambda) = (\eta_1(\omega, \lambda) + i\eta_2(\omega, \lambda) - (1 + i\gamma)|z|^2)z + y,$$

where $z \in \mathbf{C}$, γ is a real constant, $y \in \mathbf{C}$ represents the small periodic forcing, and

$$\eta_1(\omega, \lambda) = \lambda + \mathcal{O}((\omega, \lambda)^2), \quad \eta_2(\omega, \lambda) = \omega + \mathcal{O}((\omega, \lambda)^2).$$

We rewrite the equation $\Psi = 0$ as

$$(\eta_1(\omega, \lambda) + i\eta_2(\omega, \lambda) - (1 + i\gamma)|z|^2)z = -y. \tag{1.7}$$

Taking the norm of both sides of (1.7) yields

$$H(R; \omega, \lambda, \varepsilon) \equiv (1 + \gamma^2)R^3 - 2(\eta_1 + \gamma\eta_2)R^2 + (\eta_1^2 + \eta_2^2)R - \varepsilon^2 = 0, \tag{1.8}$$

where $R = |z|^2$ and $\varepsilon = |y|$. Thus, to find the number of all small amplitude 2π-periodic solutions to (1.5), it suffices to look at the number of zeros of H.

Our goal is to find the bifurcation diagrams of solutions R versus bifurcation parameter ω for different values of λ and ε. Since, by (1.8), H has the same values for $(\gamma, \eta_1, \eta_2, \varepsilon)$ and $(-\gamma, \eta_1, -\eta_2, \varepsilon)$, we may assume that γ is positive. The bifurcation diagrams for zeros of H are shown in Figure 1. They are obtained by finding those curves in the (λ, ε) parameter plane where the bifurcation diagrams are degenerate, that is, where either *hysteresis* or *bifurcation* occurs. It is shown in [10] that parameter values on these varieties are precisely the points where the bifurcation diagrams of R versus ω change qualitatively. We recall from [10] that *hysteresis points* are defined by

$$H = H_R = H_{RR} = 0$$

and *bifurcation points* by

$$H = H_R = H_\omega = 0.$$

Remarks on the stability of solutions. A complete discussion of the stability of the periodic solutions that we have found is beyond the scope of this paper. To begin, the methods of Liapunov–Schmidt reduction and $\mathbf{S}^1$-equivariant singularity theory that we use do not necessarily preserve the asymptotic stability of solutions. More important, the normal form that we prove suffices for the study of existence of solutions does not necessarily suffice for the study of stability and secondary dynamic bifurcations. We will see why when we discuss the stability of periodic solutions in the normal form equations.

More exactly, we assume that the vector field is planar, is in truncated normal form for Hopf bifurcation, and has purely sinusoidal frequency 1 forcing. Specifically, we consider the form of (1.1) given by

$$\dot{x} = (\lambda + i(1+\omega) - (1+i\gamma)|x|^2)x + \varepsilon e^{it}, \tag{1.9}$$

where $x \in \mathbf{C}$, $\varepsilon \ll 1$, and $\omega \sim 0$.

Using Hopf normal form and sinusoidal forcing guarantees that the periodic solutions are rotating waves. In particular, 2π-periodic solutions $x(t)$ of (1.9) have the form $x(t) = z(t)e^{it}$, where $z(t)$ is a solution of

$$\dot{z} = (\lambda + i\omega - (1+i\gamma)|z|^2)z + \varepsilon \equiv \Psi(z, \varepsilon, \omega, \lambda). \tag{1.10}$$

It follows that 2π-periodic solutions to (1.9) correspond to equilibria of (1.10). Most important, the stability of the periodic solutions of (1.9) is given by the stability of the associated equilibria in (1.10), and the stability of these equilibria is given by the signs of the real parts of the eigenvalues of the Jacobian $D\Psi$.

We can now investigate the stability of equilibria of $\Psi = 0$. Note that the dynamic bifurcations subdivide the regions where the five qualitatively different steady-state bifurcation diagrams shown in Figure 2 occur. The transitions between these five diagrams were determined by the hysteresis variety $\mathcal{H}$ and bifurcation variety $\mathcal{B}$ in the $\lambda\epsilon$ plane (see [10]), and these transitions change the number and arrangement of saddle-node bifurcations in the ωR plane. For parameter values of these varieties, the steady-state bifurcation diagrams have only saddle-node bifurcations, as shown in Figure 2. However, when considering stability, these same equilibria can undergo Hopf bifurcations in addition to saddle-node bifurcations. Hopf bifurcation in (1.10) leads to quasi-periodic tori in the normal form equation (1.9).

To study Hopf bifurcations we need to compute the determinant and trace of the 2×2 matrix $D\Psi$. A computation (see (F.1)) leads to

$$\begin{aligned} \det(D\Psi) &= H_R, \\ \operatorname{tr}(D\Psi) &= 2(\lambda - 2R). \end{aligned}$$

Hopf bifurcation occurs at points where $H = 0$, $\lambda - 2R = 0$, and $H_R > 0$. The eigenvalue crossing condition must hold at a generic Hopf bifurcation, that is,

$$\frac{\partial}{\partial \omega} \operatorname{tr}(D\Psi) = -4 \frac{\partial R}{\partial \omega} \neq 0. \tag{1.11}$$

This inequality is verified in Appendix F.2; it follows that there always exists a branch of periodic solutions emanating from a Hopf bifurcation in this family. However, the second Hopf genericity condition, which determines the direction of branching of the family of periodic solutions, requires the computation of third-order terms in the Hopf normal form at the bifurcation point. Hence, to complete this calculation, higher-order terms than those given in the truncated equation (1.10) are needed.

Next we discuss the transitions between bifurcation diagrams that change the number and type of Hopf bifurcations that are possible in (1.10). These transitions will be determined in principle by three possible transition varieties:

1. *Takens–Bogdanov* ($\mathcal{TB}$) variety corresponding to double zero eigenvalues of $D\Psi$,
2. *change in criticality of Hopf bifurcation* variety corresponding to the change of the Hopf bifurcation from supercritical to subcritical,
3. *double Hopf* variety corresponding to the coincidence of two Hopf bifurcations.

The double Hopf variety corresponds to Hopf points where the eigenvalue crossing condition fails and, as we discussed, does not occur in (1.10). A complete analysis of the second variety would require adding fifth-order terms in the truncated normal form (1.9) and is beyond the scope of the current paper. In a planar system, a $\mathcal{TB}$ singularity occurs when $H = \det(D\Psi) = \operatorname{tr}(D\Psi) = 0$, that is, when

$$H = H_R = \lambda - 2R = 0 \tag{1.12}$$

(see (F.2)), and these singularities can occur. The complete analysis of the $\mathcal{TB}$ singularities could require considering higher-order terms and is again beyond the scope of this paper. However, the fact that Hopf bifurcations can either be created or disappear at $\mathcal{TB}$ points can be seen from the truncated normal form. Thus, we can understand the complications involved in the discussion of stability by analyzing the $\mathcal{TB}$-variety in (1.10) in addition to the hysteresis and bifurcation varieties (where pairs of saddle-node bifurcations are created or disappear).

We see that certain changes in stability of solutions in the bifurcation diagrams in Figure 2 can lead to Hopf bifurcations and quasi-periodic motions in the forced equations and presumably to homoclinic orbits connecting a periodic solution to itself. Breaking of normal form and the associated $\mathbf{S}^1$ symmetry can lead to yet more complicated dynamics.

Theorem 1.2. *For fixed $\gamma > 0$, λ, and ε, all possible bifurcation diagrams of $\Psi = 0$ are shown in Table 1, where*

$$C_1 \approx 0.06 \quad < \quad C_2 = \frac{1}{\sqrt{3}} \approx 0.58 \quad < \quad C_3 = \frac{11}{3\sqrt{15}} \approx 0.95 \quad < \quad C_4 \approx 5.66.$$

Table 1

Bifurcation diagrams for fixed γ in the $\lambda\varepsilon$ plane. Regions I–V *refer to labels in Figures 4–8.*

γ	Region I	Region II	Region III	Region IV	Region V
$0 < \gamma < C_1$	I(a,b)	II(b)	III(a,b,c)		V(b)
$C_1 < \gamma < C_3$	I(a,b)	II(b,c)	III(b,c)		V(b)
$C_3 < \gamma < \sqrt{3}$	I(a,b)	II(b,c)	III(b)		V(a,b)
$\sqrt{3} < \gamma < C_4$	I(a)	II(a,b,c)		IV(a)	V(a,b)
$C_4 < \gamma$	I(a)	II(a,b,c)		IV(a,b)	V(b)

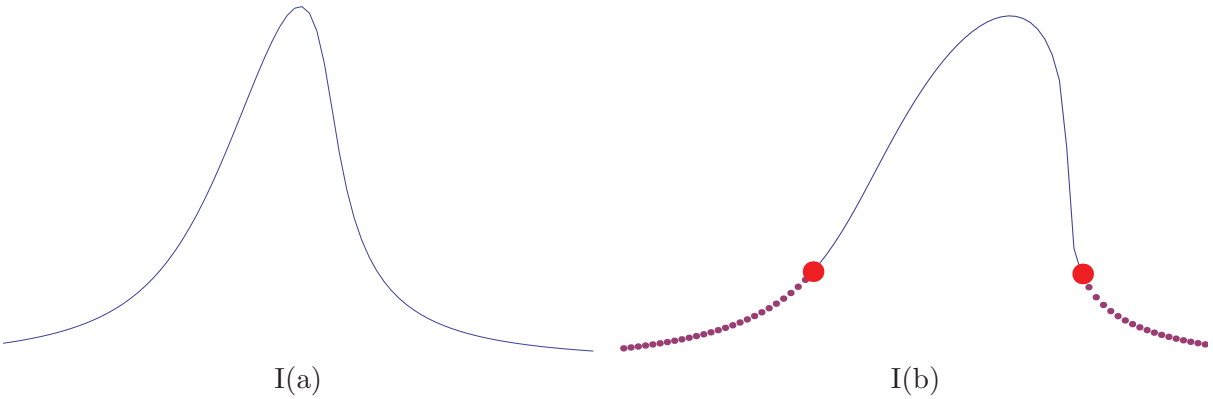

Figure 4. *Bifurcation diagrams of type* I *where ε is a function of ω in $\Psi = 0$ (1.10). There are two types of equilibria: sinks (solid blue curve) and sources (dotted purple curve). Red dots indicate changes in stability.*

The proof of Theorem 1.2 is given in Appendix F. Note also that there is a transition between diagrams I(a) and I(b) (see Figure 4) that is a nonlocal transition. This happens when the Hopf bifurcation that signifies a change from a source to a sink goes to ∞ as λ decreases to 0. This nonlocal transition also occurs in the change between diagrams II(a) and II(b) (see Figure 5). The regions where different bifurcation diagrams occur as a function of γ are given in Figure 9.

Structure of the paper. We now describe the structure of this paper. In section 2, we use Liapunov–Schmidt reduction and $\mathbf{S}^1$ phase-shift symmetry to simplify the infinite-dimensional problem of solving for the 2π-periodic solutions of (1.5) on loop space to the problem of solving for the zeros of an equivariant map $\psi : \mathbf{C} \times \mathbf{C} \times \mathbf{R}^2 \to \mathbf{C}$. See Proposition 2.1. In section 3, we introduce $\mathbf{S}^1$-singularity theory with parameter symmetry, compute the restricted tangent space of $\psi(\cdot, \cdot, 0, 0)$, and find a normal form for $\psi(\cdot, \cdot, 0, 0)$. In section 4, we use the universal unfolding theorem (stated in Theorem 4.7) to derive a universal unfolding of the normal form of $\psi(\cdot, \cdot, 0, 0)$ (Proposition 4.5). In section 5 we show that by analyzing the normal form for this universal unfolding, we can obtain the structure of the zero set of ψ and capture all possible bifurcation diagrams of ψ with bifurcation parameter ω. As desired, the universal unfolding depends on the two parameters ε and λ. To determine the bifurcation diagrams in ω, we need to compute the transition variety in the $\lambda\varepsilon$ plane; these calculations use the universal unfolding theorem and are described in section 6. The descriptions of various calculations are given in the six appendices.

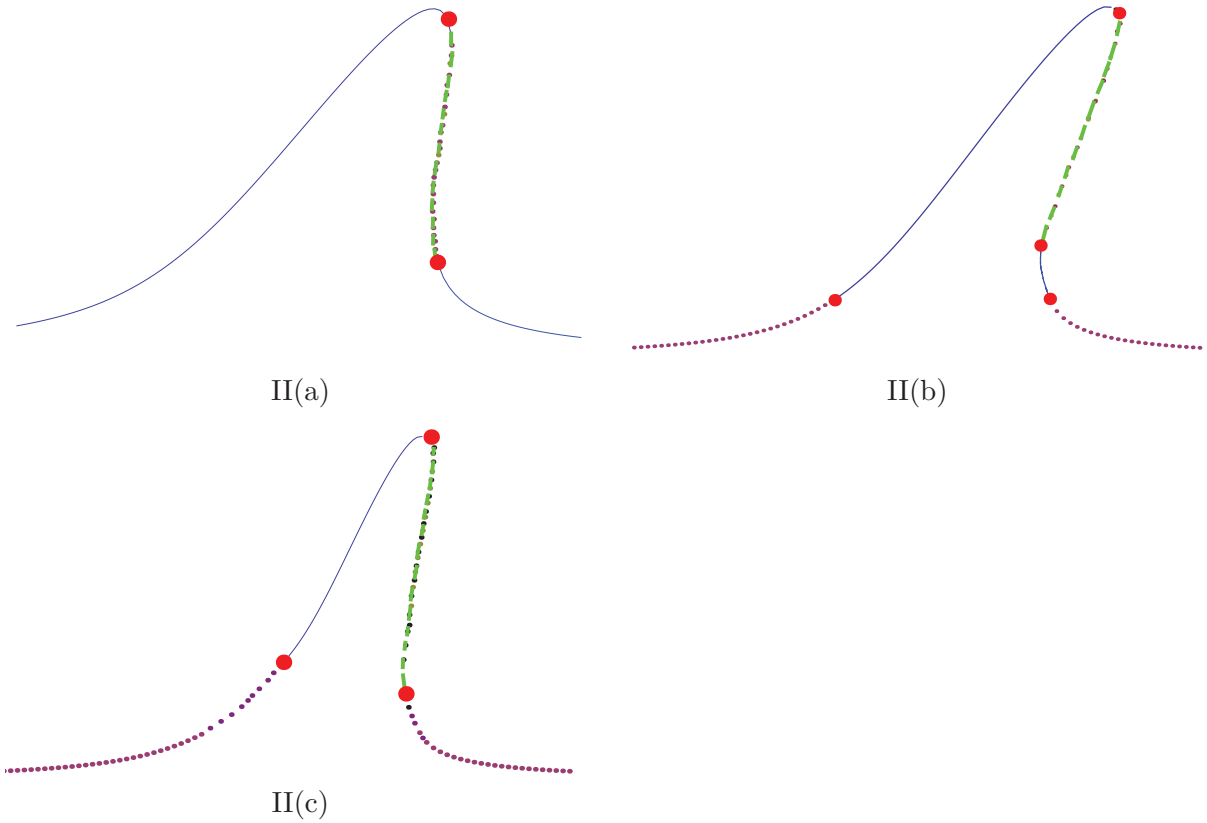

Figure 5. *Bifurcation diagrams of type* II *where ε is a function of ω in $\Psi = 0$ (1.10). There are three types of equilibria: sink (solid blue curve), saddle (thick dashed green curve), and source (dotted purple curve). Red dots indicate changes in stability.*

2. Liapunov–Schmidt reduction.

In this section, we use Liapunov–Schmidt reduction to simplify the bifurcation problem to a low-dimensional $\mathbf{S}^1$-equivariant problem.

Using loop space arguments as in the Liapunov–Schmidt proof for Hopf bifurcation, we can find 2π-periodic solutions to (1.5) by searching for zeros of the operator

$$N(x, G, \omega, \lambda) \equiv \frac{dx}{ds} - F(x, G(s), \omega, \lambda), \tag{2.1}$$

where 2π-periodic $G(s)$ and $\omega, \lambda \in \mathbf{R}$ are all parameters. We denote the space of continuous 2π-periodic functions by $\mathcal{C}_{2\pi}$, and the subspace of continuously differentiable 2π-periodic functions by $\mathcal{C}^1_{2\pi}$. It follows that $N : \mathcal{C}^1_{2\pi} \times \mathcal{C}_{2\pi} \times \mathbf{R}^2 \to \mathcal{C}_{2\pi}$. Since in this study we fix G and only allow phase shifts in G, we can identify the forcing space with $\mathbf{C}$ via the mapping

$$y \mapsto G = \mathrm{Re}(ye^{is}). \tag{2.2}$$

Thus, N is restricted to be

$$N : \mathcal{C}^1_{2\pi} \times \mathbf{C} \times \mathbf{R}^2 \to \mathcal{C}_{2\pi}.$$

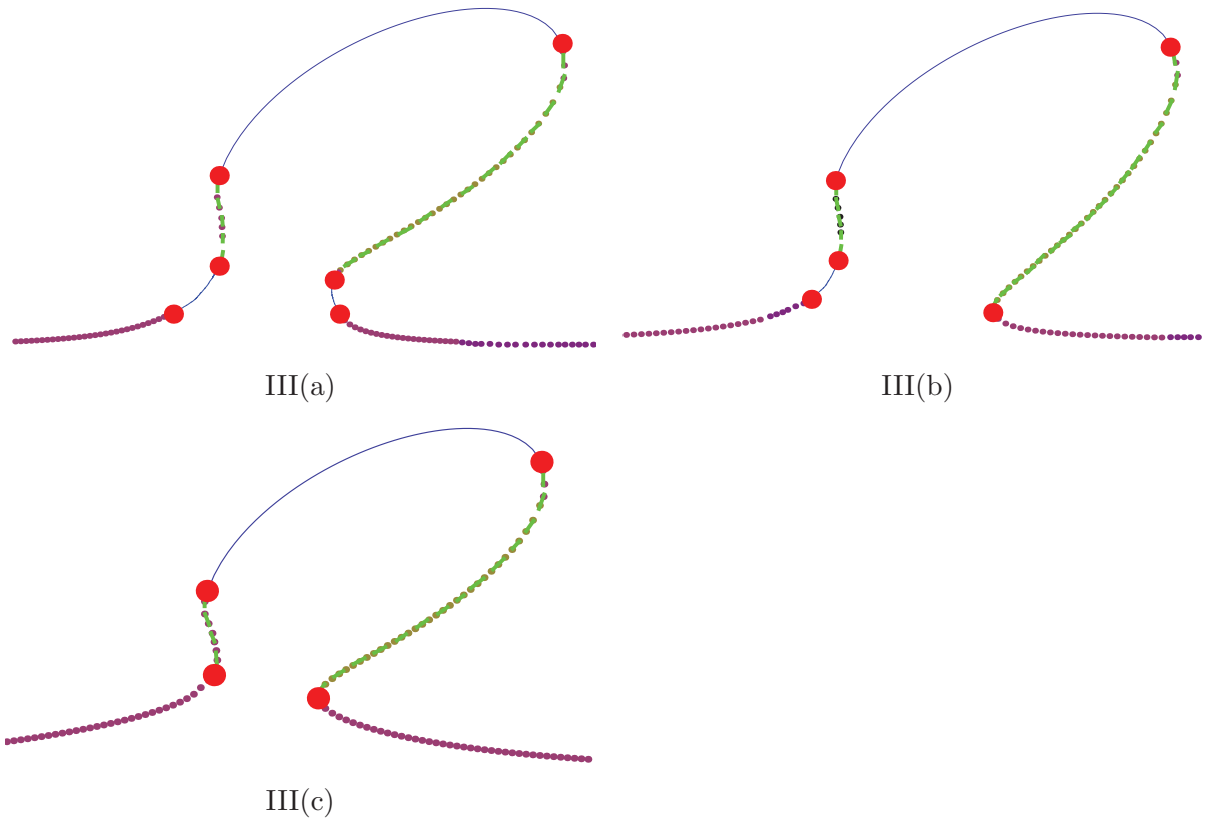

Figure 6. *Bifurcation diagrams of type* III *where* ε *is a function of* ω *in* $\Psi = 0$ (1.10). *There are three types of equilibria: sink (solid blue curve), saddle (thick dashed green curve), and source (dotted purple curve). Red dots indicate changes in stability.*

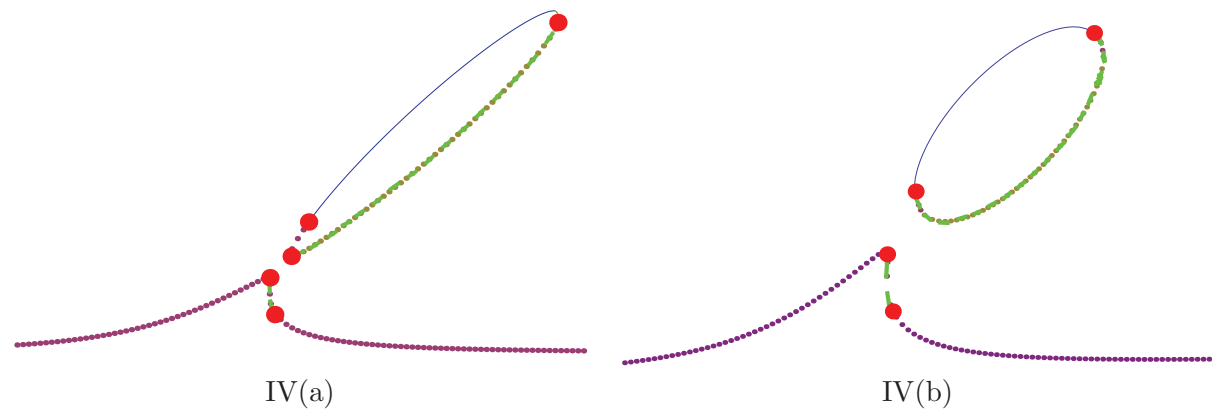

Figure 7. *Bifurcation diagrams of type* IV *where* ε *is a function of* ω *in* $\Psi = 0$ (1.10). *There are three types of equilibria: sink (solid blue curve), saddle (thick dashed green curve), and source (dotted purple curve). Red dots indicate changes in stability.*

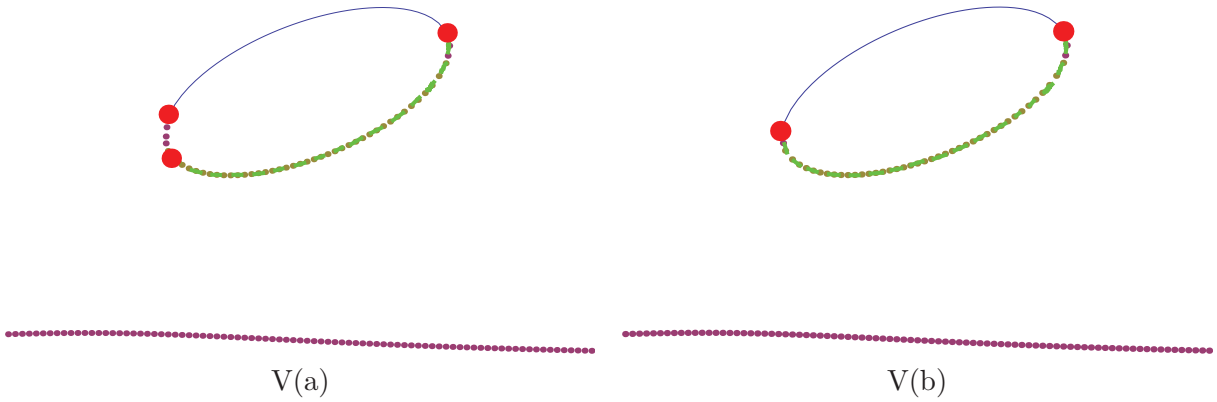

Figure 8. *Bifurcation diagrams of type* V *where* ε *is a function of* ω *in* $\Psi = 0$ (1.10). *There are three types of equilibria: sink (solid blue curve), saddle (thick dashed green curve), and source (dotted purple curve). Red dots indicate changes in stability.*

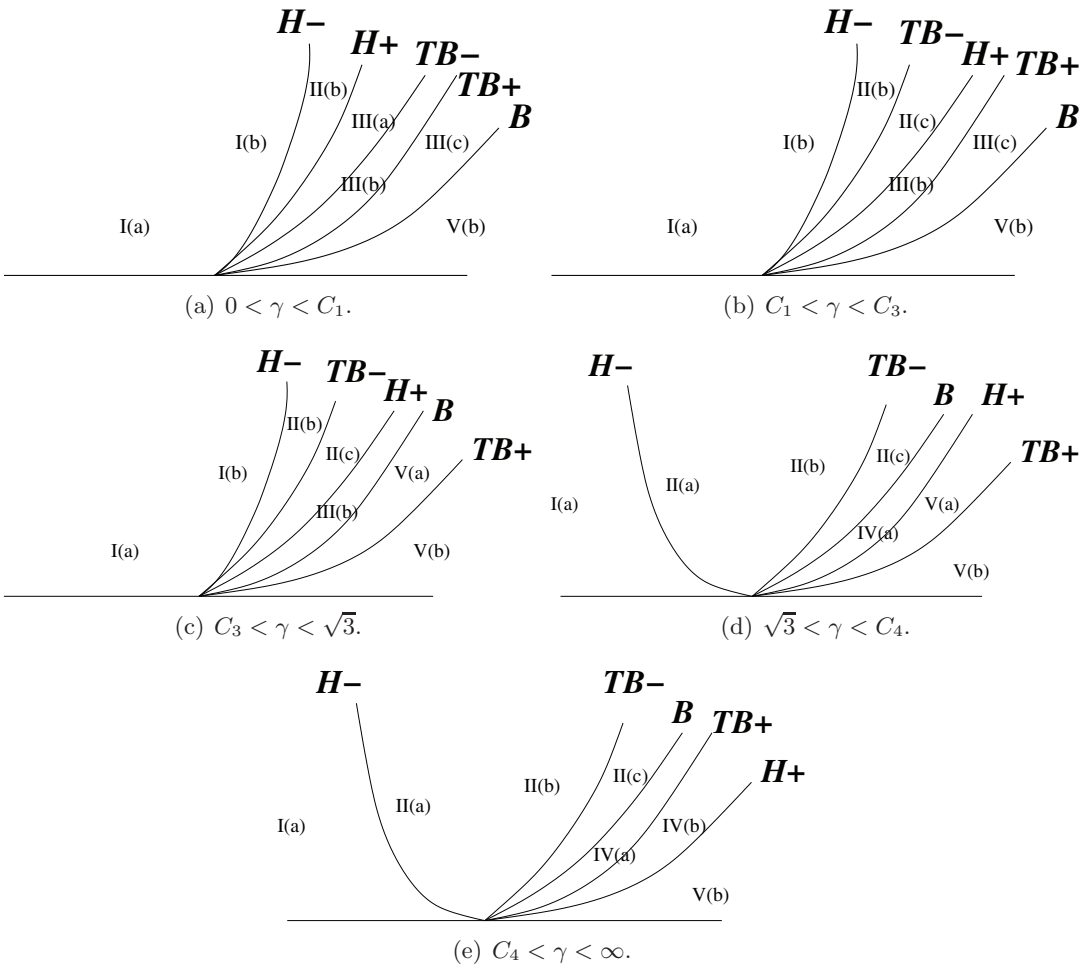

Figure 9. *Regions of bifurcation diagrams depending on* γ. *Bifurcation diagrams are found in Figures* 4–8.

We now discuss the symmetry properties of the mapping N. The circle group $\mathbf{S}^1 = [0, 2\pi)$ acts on $\mathcal{C}_{2\pi}$ by a phase shift, that is,

$$\theta f(s) = f(s+\theta) \tag{2.3}$$

for any $\theta \in \mathbf{S}^1$ and $f \in \mathcal{C}_{2\pi}$. So we have

$$\theta x(s) = x(s+\theta) \quad \text{and} \quad \theta G(s) = G(s+\theta) = \mathrm{Re}(ye^{is+i\theta}) = \mathrm{Re}((e^{i\theta}y)e^{is}).$$

It follows that

$$\begin{aligned} \theta N(x(s), G(s), \omega, \lambda) &= N(x(s+\theta), G(s+\theta), \omega, \lambda) \\ &= N(\theta x(s), \theta G(s), \omega, \lambda) \end{aligned} \tag{2.4}$$

and that the action of θ on y is

$$\theta y = e^{i\theta} y; \tag{2.5}$$

that is, θ acts on y by a counterclockwise rotation of angle θ. Note that (2.4) just states that N is $\mathbf{S}^1$-equivariant.

Next, we apply Liapunov–Schmidt reduction [10] to the restricted problem $N = 0$ and then verify that $\mathbf{S}^1$-equivariance is preserved through the reduction [18]. Thus we obtain the following claim.

Proposition 2.1. *There exists an $\mathbf{S}^1$-equivariant function ψ: $\mathbf{C} \times \mathbf{C} \times \mathbf{R}^2 \to \mathbf{C}$ such that zeros of ψ are in one-to-one correspondence with small 2π-periodic solutions of system (1.5).*

Proof. It suffices to show existence of an $\mathbf{S}^1$-equivariant function ψ: $\mathbf{C} \times \mathbf{C} \times \mathbf{R}^2 \to \mathbf{C}$ whose zeros are in one-to-one correspondence with $N : \mathcal{C}^1_{2\pi} \times \mathbf{C} \times \mathbf{R}^2 \mapsto \mathcal{C}_{2\pi}$. We use the standard proof of $\mathbf{S}^1$-equivariance in Hopf bifurcation (see [10, 11]) to sketch the proof. Note that $L \equiv (d_x N)_{0,0,0,0}$ does not depend on the forcing function (that is, $\varepsilon = 0$ when taking the derivative). It follows from the proof of Hopf bifurcation that $\ker L$ is two-dimensional, the implicit function determined in Liapunov–Schmidt reduction is $\mathbf{S}^1$-equivariant, and the reduced function is also $\mathbf{S}^1$-equivariant. Note, however, that in this lemma $\mathbf{S}^1$-equivariance includes the action on the forcing parameter space. The smooth dependence of solutions on parameters in the implicit function theorem completes the proof. ∎

The remainder of this section discusses the structure of the reduced mapping ψ that follows directly from symmetry and Hopf bifurcation.

2.1. Invariants and equivariants. Recall that a function $\mu : \mathbf{C} \times \mathbf{C} \to \mathbf{R}$ is $\mathbf{S}^1$-*invariant* if

$$\mu(\theta z, \theta y) = \mu(z, y)$$

for all $z, y \in \mathbf{C}$ and $\theta \in \mathbf{S}^1$. In [18] we prove the following lemmas.

Lemma 2.2. *If $\mu : \mathbf{C} \times \mathbf{C} \to \mathbf{R}$ is $\mathbf{S}^1$-invariant, then there exists a mapping ρ such that*

$$\mu(z, y) = \rho(v_1, v_2, v_3, v_4),$$

where $z, y \in \mathbf{C}$ and

$$\begin{aligned} v_1 &= z\bar{z}, & v_2 &= y\bar{y}, \\ v_3 &= z\bar{y} + \bar{z}y, & v_4 &= i(z\bar{y} - \bar{z}y). \end{aligned} \tag{2.6}$$

Moreover, μ can be expressed in the following unique way:

$$\rho = f_1(v_1, v_2, v_3) + v_4 f_2(v_1, v_2, v_3),$$

where $f_1, f_2 : \mathbf{R}^3 \to \mathbf{R}$.

So, we can write an $\mathbf{S}^1$-equivariant function in the form (2.7).

Lemma 2.3. *Given any $\mathbf{S}^1$-equivariant function $\zeta : \mathbf{C}\times\mathbf{C} \to \mathbf{C}$, there exist unique functions $p, q : \mathbf{R}^3 \to \mathbf{C}$ such that*

$$\zeta(z, y) = p(v_1, v_2, v_3)z + q(v_1, v_2, v_3)y. \tag{2.7}$$

Hence, we can simply denote ζ by $[p^R, p^I, q^R, q^I]$, where p^R, p^I, q^R, q^I are real and imaginary parts of p, q, respectively.

2.2. Lower-order terms in ψ. Let $\psi(z, y, \omega, \lambda)$, where $z, y \in \mathbf{C}$, be the reduced function obtained in Proposition 2.1. We will show in Proposition 4.5 that ψ is a general form if $d_z(\psi_\omega)(0)$ and $d_z(\psi_\lambda)(0)$ are linearly independent over $\mathbf{R}$. However, we prove in the following proposition that the linear independence follows naturally.

Proposition 2.4. *Assume that the system (1.5) satisfies the eigenvalue conditions (1.6). Then*

$$\begin{aligned} d_z(\psi_\omega)(0) &= -i, \\ d_z(\psi_\lambda)(0) &= -\sigma_\lambda(0) + i\kappa_\lambda(0), \end{aligned} \tag{2.8}$$

where $\sigma_\lambda(0) \neq 0$. Hence, $d_z(\psi_\omega)(0)$ and $d_z(\psi_\lambda)(0)$ are linearly independent over $\mathbf{R}$.

Proof. We will show in Lemma 2.3 that, by $\mathbf{S}^1$-equivariance, ψ has the form

$$\psi(z, y, \omega, \lambda) = p(|z|^2, |y|^2, z\bar{y} + \bar{y}z, \omega, \lambda)z + q(|z|^2, |y|^2, z\bar{y} + \bar{y}z, \omega, \lambda)y, \tag{2.9}$$

where $z, y \in \mathbf{C}$ and $p, q \in \mathbf{C}$. Since $d_z(\psi_\omega)(0)$ and $d_z(\psi_\omega)(0)$ are independent of the forcing term y, in this proof for Proposition 2.4 we can simply set $y = 0$. By (2.9), we have that

$$\psi(z, 0, \omega, \lambda) = p(|z|^2, 0, 0, \omega, \lambda)z.$$

It follows that

$$d_z(\psi_\omega)(0) = p_\omega(0) \quad \text{and} \quad d_z(\psi_\lambda)(0) = p_\lambda(0).$$

By Lemma 2.5, (2.8) holds. ∎

Lemma 2.5. *p satisfies*

$$p_\omega(0) = -i \tag{2.10}$$

and

$$p_\lambda(0) = -\frac{1}{2}(\bar{d}^T A_\lambda(0)c) = -\sigma_\lambda(0) + i\kappa_\lambda(0), \tag{2.11}$$

where c and d are eigenvectors of $A(0)$ and $A(0)^T$ associated with i and $-i$, respectively.

This lemma can be proved by using the same idea as that in [10] for the standard Hopf bifurcation. In fact, from the form (1.4) for the forced system, we see that as $G = 0$ the problem (1.5) is exactly the problem of the standard Hopf bifurcation for $\omega = 0$. Thus, (2.11) follows simply from the results for the standard Hopf bifurcation. Equation (2.10) can be verified by just noting that ω plays exactly the same role in this bifurcation as the time rescaling parameter τ does in standard Hopf bifurcation (see [10]).

3. Normal form for $\psi(\cdot,\cdot,0,0)$. Proposition 2.1 shows that there exists a function $\psi : \mathbf{C}\times\mathbf{C}\times\mathbf{R}^2 \to \mathbf{C}$ such that near the origin the $\mathbf{S}^1$-orbits of zeros of ψ are in one-to-one correspondence with small 2π-periodic solutions to (1.5). To determine the zeros of ψ, we first derive a normal form for the $\mathbf{S}^1$-equivariant mapping $\psi_0(z,y) \equiv \psi(z,y,0,0)$ and then show in section 4 that ω,λ are universal unfolding parameters for ψ_0 in the $\mathbf{S}^1$-equivariant context. Finally, we use this universal unfolding to find all zeros of ψ.

To find a normal form for $\psi_0 : \mathbf{C}\times\mathbf{C}\to\mathbf{C}$, we use standard arguments in singularity theory (see [11, 3, 6]). We first find generators for the restricted tangent space $RT(\zeta,\mathbf{S}^1)$ of a general $\mathbf{S}^1$-equivariant map $\zeta : \mathbf{C}\times\mathbf{C}\to\mathbf{C}$ as a module over the ring of invariant functions. Then we compute $RT(\zeta,\mathbf{S}^1)$ and use the tangent space constant theorem (Theorem 3.3) to obtain a normal form for ζ. Thus we derive a normal form for ψ_0. Note that standard equivariant singularity theory (see [11]) is usually applied to problems with symmetry on the state variable. However, in our context, $\mathbf{S}^1$-symmetry acts on both the state variable and the parameter. So, instead of using the standard scheme, we use the results in [6], which follow from the theorems in [3]. More details are given in [18].

In subsection 3.1, we recall the notion of strong equivalence and the restricted tangent space, and state the equivariant restricted tangent space constant theorem in our context. In subsection 3.2 we calculate the restricted tangent space of an $\mathbf{S}^1$-equivariant function satisfying certain conditions and obtain a normal form for ψ_0 in subsection 3.3.

3.1. Restricted tangent spaces. Now we define strong $\mathbf{S}^1$-equivalence and the $\mathbf{S}^1$-equivariant restricted tangent space and state the equivariant restricted tangent constant theorem. Recall that

$$\vec{\mathcal{E}}_{z,y}(\mathbf{S}^1) \equiv \{\zeta : \mathbf{C}\times\mathbf{C}\to\mathbf{C} : \zeta \text{ is } \mathbf{S}^1\text{-equivariant}\},$$

where $z,y\in\mathbf{C}$.

Definition 3.1. *The mappings $\zeta,\chi\in\vec{\mathcal{E}}_{z,y}(\mathbf{S}^1)$ are* $\mathbf{S}^1$-equivalent *if there exist an $\mathbf{S}^1$-equivariant invertible change of coordinates $(z,y)\to(V(z,y),Y(y))$ and a smooth function $S(z,y)\in\mathbf{C}$ such that*

$$\zeta(z,y) = S(z,y)\chi(V(z,y),Y(y)), \tag{3.1}$$

where

$$\begin{aligned} &S(\theta z,\theta y) = S(z,y) \quad \textit{for all } \theta\in\mathbf{S}^1,\\ &S(0,0)\neq 0. \end{aligned} \tag{3.2}$$

We say that ζ and χ are strongly $\mathbf{S}^1$-equivalent *if $Y(y)\equiv y$.*

Remark 3.2. In Definition 3.1, $S(z,y)\neq 0$ in a neighborhood of $(0,0)$ since $S(0,0)\neq 0$ and S is smooth. So, (3.1) implies that

$$\zeta(z,y) = 0 \quad \text{if and only if} \quad \chi(V(z,y),Y(y)) = 0.$$

That is, the number of zeros of $\zeta(\cdot,y)$ equals the number of zeros of $\chi(V(\cdot,y),Y(y))$, which equals the number of zeros of $\chi(\cdot,Y(y))$, since $V(\cdot,y)$ is invertible. Moreover, since $Y(y)$ is invertible, $\zeta(\cdot,y)=0$ and $\chi(\cdot,y)=0$ are qualitatively the same.

Let *the* $\mathbf{S}^1$*-equivariant restricted tangent space* of ζ be

$$RT(\zeta, \mathbf{S}^1) \equiv \{S\zeta + (d_z\zeta)V : S \text{ satisfies (3.2) and } V \text{ is } \mathbf{S}^1\text{-equivariant}\}. \tag{3.3}$$

To find functions that are strongly $\mathbf{S}^1$-equivalent to ζ, we use the equivariant restricted tangent space constant theorem.

Theorem 3.3 (equivariant restricted tangent space constant theorem). *Let* $\zeta,\ r \in \vec{\mathcal{E}}_{z,y}(\mathbf{S}^1)$. *Suppose that*

$$RT(\zeta + tr, \mathbf{S}^1) = RT(\zeta, \mathbf{S}^1) \tag{3.4}$$

for all $t \in [0,1]$. *Then* $\zeta + tr$ *is strongly* $\mathbf{S}^1$*-equivalent to* ζ *for all* $t \in [0,1]$.

The proof of the theorem is similar to the proof in [11, Chapter XIV, section 2].

3.2. Calculation of $RT(\psi_0, \mathbf{S}^1)$. By Theorem 3.3, to find a normal form for ψ_0, we need to compute the $\mathbf{S}^1$-equivariant restricted tangent space of ψ_0. We first calculate the $RT(\zeta, \mathbf{S}^1)$ for $\zeta \in \vec{\mathcal{E}}_{z,y}(\mathbf{S}^1)$ satisfying (3.6) (see Proposition 3.4). Then we apply Proposition 3.4 to ψ_0.

For any $\zeta \in \vec{\mathcal{E}}_{z,y}(\mathbf{S}^1)$, by Lemma 2.3, there exist functions $p, q : \mathbf{R}^3 \to \mathbf{C}$ such that

$$\zeta(z,y) = p(v_1, v_2, v_3)z + q(v_1, v_2, v_3)y, \tag{3.5}$$

where v_1, v_2, v_3 are defined in (2.6). Let $\mathcal{E}$ be the space of all functions $f : \mathbf{R}^3 \to \mathbf{R}$ that are smooth near the origin. And let

$$\mathcal{M} = \{f \in \mathcal{E} : f(0,0,0) = 0\}$$

and

$$\mathcal{N} = [\mathcal{M}, \mathcal{M}, \mathcal{E}, \mathcal{E}].$$

Proposition 3.4. *Assume that* ζ *has the form* (3.5) *and satisfies*

$$\begin{array}{ll} \text{(i)} & p(0,0,0) = 0, \\ \text{(ii)} & p_{v_1}(0,0,0) \neq 0, \\ \text{(iii)} & q(0,0,0) \neq 0. \end{array} \tag{3.6}$$

Then

$$RT(\zeta, \mathbf{S}^1) = \mathcal{N}. \tag{3.7}$$

Proof. See Appendix B. ∎

Since $\psi_0 \in \vec{\mathcal{E}}_{z,y}(\mathbf{S}^1)$, Proposition 3.4 is also true for ψ_0; i.e.,

$$RT(\psi_0, \mathbf{S}^1) = \mathcal{N} \tag{3.8}$$

if ψ_0 satisfies (3.6). In fact, ψ_0 satisfies the first two conditions in (3.6) by the standard Hopf bifurcation and the last by the assumption about the forcing (more precisely, its minimal period is 2π, so the linear term in y does not vanish in the normal form).

3.3. Normal form for ψ_0. Now we can prove that h in (3.9) is a normal form for any $\zeta \in \vec{\mathcal{E}}_{z,y}(\mathbf{S}^1)$ which satisfies (3.6), so also for ψ_0.

Proposition 3.5. *If ζ in (3.5) satisfies (3.6), then ζ is strongly $\mathbf{S}^1$-equivalent to*

$$h(z,y) = -|z|^2 z + y. \tag{3.9}$$

Proof. Use Taylor's theorem so that

$$\begin{aligned}\zeta_t = {} & [p^R_{v_1}(0)v_1, p^I_{v_1}(0)v_1, q^R(0), q^I(0)] \\ & + t[p^R_{v_2}(0)v_2 + p^R_{v_3}(0)v_3 + r_1, p^I_{v_2}(0)v_2 + p^I_{v_3}(0)v_3 + r_2, r_3, r_4],\end{aligned}$$

where $r_1, r_2 \in \mathcal{M}^2$ and $r_3, r_4 \in \mathcal{M}$ are remainder terms chosen so that $\zeta_1 = \zeta$. Proposition 3.4 gives rise to

$$RT(\zeta_t, \mathbf{S}^1) = RT(\tilde{h}, \mathbf{S}^1) = \mathcal{N}$$

for all $t \in [0,1]$, where $\tilde{h} = [p^R_{v_1}(0)v_1, p^I_{v_1}(0)v_1, q^R(0), q^I(0)]$. By Theorem 3.3, ζ_t is strongly $\mathbf{S}^1$-equivalent to $\tilde{h}$ for all $t \in [0,1]$. So is ζ_1. However, $\tilde{h}$ is strongly $\mathbf{S}^1$-equivalent to h since

$$h(z,y) = S(z,y)\tilde{h}(V(z,y), y),$$

where

$$S(z,y) = \frac{1}{q}(0) \neq 0, \qquad V(z,y) = Bz,$$

and

$$B = -\frac{|p_{v_1}|^{2/3} q}{p_{v_1}|q|^{2/3}}(0) \neq 0$$

by (3.6). By the transitivity of strong $\mathbf{S}^1$-equivalence, ζ_1 is strongly $\mathbf{S}^1$-equivalent to h, where $\zeta_1 = \zeta$. ∎

Note that, by Proposition 3.4 and the proof of Proposition 3.5, we have

$$RT(h, \mathbf{S}^1) = \mathcal{N}. \tag{3.10}$$

4. Universal unfoldings of h. In the previous section, we obtain a normal form h for ψ with $\omega = \lambda = 0$. To determine the number of zeros of ψ for different values of ω and λ, we find a *universal unfolding* of h that includes all possible perturbations of h up to $\mathbf{S}^1$-equivalence, and show that qualitatively this universal unfolding has the same set of numbers of possible zeros as ψ.

Let $\zeta \in \vec{\mathcal{E}}_{z,y}(\mathbf{S}^1)$ and $\Psi \in \vec{\mathcal{E}}_{z,y,\mu}(\mathbf{S}^1)$, where $\mu = (\mu_1, \ldots, \mu_k) \in \mathbf{R}^k$. We call Ψ a *k-parameter unfolding* of ζ if

$$\Psi(z,y,0) = \zeta(z,y).$$

Definition 4.1. *Let $\Psi(z,y,\mu), \Phi(z,y,\eta)$ be unfoldings of $\zeta \in \vec{\mathcal{E}}_{z,y}(\mathbf{S}^1)$, where $\mu \in \mathbf{R}^k$ and $\eta \in \mathbf{R}^l$. Φ* factors through *Ψ if there exist smooth mappings S, V, Υ such that*

$$\Phi(z,y,\eta) = S(z,y,\eta)\Psi(V(z,y,\eta), y, \Upsilon(\eta)), \tag{4.1}$$

where

$$\begin{array}{ll} S(\theta z, \theta y, \eta)\theta = \theta S(z, y, \eta), & S(z, y, 0) = I, \\ V(\theta z, \theta y, \eta) = \theta V(z, y, \eta), & V(z, y, 0) = z, \\ \Upsilon(0) = 0. & \end{array} \tag{4.2}$$

Remark 4.2. It follows from Definition 3.1 that $\Phi(\cdot, y, \eta)$ and $\Psi(\cdot, y, \Upsilon(\eta))$ are strongly $\mathbf{S}^1$-equivalent, where $\Upsilon : \mathbf{R}^l \to \mathbf{R}^k$. It also follows from Remark 3.2 that $\Phi(\cdot, y, \eta)$ and $\Psi(\cdot, y, \Upsilon(\eta))$ have the same number of zeros.

Definition 4.3. *An unfolding* Ψ *of* $\zeta \in \vec{\mathcal{E}}_{z,y}(\mathbf{S}^1)$ *is* versal *if any unfolding of* ζ *factors through* Ψ. *We call a versal unfolding of* ζ universal *if the unfolding depends on the minimum number of parameters.*

In this section we will show the following.

Proposition 4.4. *h has a universal unfolding*

$$\Phi(z, y, \eta_1, \eta_2) = (\eta_1 + i\eta_2 - |z|^2)z + y, \tag{4.3}$$

where $\eta_1, \eta_2 \in \mathbf{R}$.

We also find the next result.

Proposition 4.5. *ψ is a universal unfolding of ψ_0.*

Moreover, the structure of zero sets of ψ can be obtained via Φ.

Proposition 4.6. *There exists $\eta(\omega, \lambda) = (\eta_1(\omega, \lambda), \eta_2(\omega, \lambda))$ such that $\Phi(z, y, \eta)$ and $\psi(z, y, \omega, \lambda)$ have the same possible number of zeros. Moreover, $\eta_\omega(0, 0)$ and $\eta_\lambda(0, 0)$ are linearly independent over $\mathbf{R}$.*

Proof. We have known from section 3 that ψ_0 is strongly $\mathbf{S}^1$-equivalent to h. It follows that there exist smooth mapping S and invertible $\mathbf{S}^1$-equivariant mapping V such that

$$\psi_0(z, y) = S(z, y)h(V(z, y), y),$$

where S satisfies (3.2). Since $\Phi(z, y, 0) = h(z, y)$ by (4.3),

$$S(z, y)\Phi(V(z, y), y, 0) = S(z, y)h(V(z, y), y) = \psi_0(z, y).$$

It follows that

$$\tilde{\Phi}(z, y, \eta) \equiv S(z, y)\Phi(V, y, \eta)$$

is a universal unfolding of ψ_0 by the fact that Φ is a universal unfolding of h. But, ψ is an unfolding of ψ_0. Hence, ψ factors through $\tilde{\Phi}$. So, there exist smooth mappings T, U, η such that

$$\psi(z, y, \omega, \lambda) = T(z, y, \omega, \lambda)\tilde{\Phi}(U(z, y, \omega, \lambda), y, \eta(\omega, \lambda)),$$

where T, U, η satisfy (4.2). Since T is invertible near $(\omega, \lambda) = (0, 0)$ by the fact that $T(z, y, 0, 0) = I$, we have

$$\psi(z, y, \omega, \lambda) = 0 \quad \Leftrightarrow \quad \tilde{\Phi}(U, y, \eta) = 0,$$

i.e.,

$$\psi = 0 \quad \Leftrightarrow \quad S(U, y)\Phi(V(U, y), y, \eta(\omega, \lambda)) = 0.$$

Since the smooth mapping $S(0,0) \neq 0$ and $U(0) = 0$, then $\psi = 0$ if and only if

$$\Phi(V(U,y), y, \eta(\omega,\lambda)) = 0,$$

where y, ω, λ are close to 0. But, $\Phi(V(U,y), y, \eta)$ has the same number of zeros as $\Phi(z,y,\eta)$ since U, V are invertible. Therefore, the number of zeros of $\psi(z,y,\omega,\lambda)$ is the same as for $\Phi(z,y,\eta(\omega,\lambda))$. Moreover, since ψ and Φ are both 2-parameter universal unfoldings by Propositions 4.4 and 4.5, $\eta_\omega(0,0)$ and $\eta_\lambda(0,0)$ are linearly independent over $\mathbf{R}$ for the generality. ■

By Proposition 4.6 and (4.3) we need only find the zeros of

$$\Phi(z,y,\eta) = (\eta_1(\omega,\lambda) + i\eta_2(\omega,\lambda) - |z|^2)z + y \tag{4.4}$$

to obtain the number of zeros of ψ.

It remains to prove Propositions 4.4 and 4.5. Let $\Phi \in \vec{\mathcal{E}}_{z,y,\eta}(\mathbf{S}^1)$ be an l-parameter unfolding of h, where h is given in (3.9). Then

$$\Phi(z,y,\eta) = h(z,y) + \sum_{i=1}^{l} \eta_i r_i(z,y), \tag{4.5}$$

where $r_i \in \vec{\mathcal{E}}_{z,y}(\mathbf{S}^1)$. Suppose that $\Psi \in \vec{\mathcal{E}}_{z,y,\mu}(\mathbf{S}^1)$ is a k-parameter versal unfolding of h. By Definitions 4.1 and 4.3, Φ factors through Ψ, and they satisfy (4.1).

Taking partial derivatives of (4.1) and (4.5) with respect to η_i at $\eta = 0$ yields that

$$r_i(z,y) = \frac{\partial S}{\partial \eta_i}(z,y,0)h(z,y) + h_z(z,y)\frac{\partial V}{\partial \eta_i}(z,y,0) + \sum_{j=1}^{k} \frac{\partial \Psi}{\partial \mu_j}(z,y,0)\frac{\partial \Upsilon_j}{\partial \eta_i}(0). \tag{4.6}$$

Hence,

$$r_i(z,y) \in RT(h,\mathbf{S}^1) + \mathbf{R}\left\{\frac{\partial \Psi}{\partial \mu_1}(z,y,0), \ldots, \frac{\partial \Psi}{\partial \mu_k}(z,y,0)\right\}$$

for any $r_i(z,y) \in \vec{\mathcal{E}}_{z,y}(\mathbf{S}^1)$. So,

$$\vec{\mathcal{E}}_{z,y}(\mathbf{S}^1) = RT(h,\mathbf{S}^1) + \mathbf{R}\left\{\frac{\partial \Psi}{\partial \mu_1}(z,y,0), \ldots, \frac{\partial \Psi}{\partial \mu_k}(z,y,0)\right\}. \tag{4.7}$$

Conversely, if (4.7) holds, then Ψ is a versal unfolding of h [11]. Thus, we have the following claim.

Theorem 4.7 (unfolding theorem). *Let $\Psi \in \vec{\mathcal{E}}_{z,y,\mu}(\mathbf{S}^1)$ be a k-parameter unfolding of $h \in \vec{\mathcal{E}}_{z,y}(\mathbf{S}^1)$. Then Ψ is a versal unfolding of h if and only if (4.7) holds.*

Proposition 4.4 follows from Theorem 4.7 and (3.10), since Φ satisfies (4.7).

Next, we prove Proposition 4.5 by applying the idea [10] used for the recognition problems of universal unfoldings. Recall that a submodule $\mathcal{J} \subset \vec{\mathcal{E}}_{z,y}(\mathbf{S}^1)$ is *intrinsic* if for any $\zeta, \chi \in \vec{\mathcal{E}}_{z,y}(\mathbf{S}^1)$ the fact that $\zeta \in \mathcal{J}$ is strongly $\mathbf{S}^1$-equivalent to χ implies that $\chi \in \mathcal{J}$. We denote $\mathcal{J}$ by $Itr\ (\vec{\mathcal{E}}_{z,y}(\mathbf{S}^1))$. For any $\zeta \in \vec{\mathcal{E}}_{z,y}(\mathbf{S}^1)$, we define

$$J\zeta = \sum_{\mu} \frac{1}{\mu!} D^\mu \zeta(0) z^{\mu_1} \bar{z}^{\mu_2} y^{\mu_3} \bar{y}^{\mu_4}, \tag{4.8}$$

where each $z^{\mu_1}\bar{z}^{\mu_2}y^{\mu_3}\bar{y}^{\mu_4} \in [Itr\ RT(\zeta, \mathbf{S}^1)]^{\perp}$.

Proof of Proposition 4.5. By (3.10), we have that

$$RT(h, \mathbf{S}^1) = \mathcal{N} = Itr\ RT(h, \mathbf{S}^1).$$

So, by Lemma 4.2 [10], ψ is a universal unfolding of ψ_0 if and only if

$$[Itr\ RT(h, \mathbf{S}^1)]^{\perp} = \mathbf{R}[1,0,0,0] + \mathbf{R}[0,1,0,0] = \mathbf{R}\{J\psi_\omega, J\psi_\lambda\}, \tag{4.9}$$

where by definition (4.8)

$$J\psi_\omega = d_z(\psi_\omega)(0)z = [\mathrm{Re}(d_z(\psi_\omega)(0)), \mathrm{Im}(d_z(\psi_\omega)(0)), 0, 0]$$

and

$$J\psi_\lambda = d_z(\psi_\lambda)(0)z = [\mathrm{Re}(d_z(\psi_\lambda)(0)), \mathrm{Im}(d_z(\psi_\lambda)(0)), 0, 0].$$

Hence, (4.9) holds only when $d_z(\psi_\omega)(0)$ and $d_z(\psi_\lambda)(0)$ are linearly independent over $\mathbf{R}$. Note that we have proved this linear independence in Proposition 2.4. Thus, we are done. ∎

5. The bifurcation problem. We want to find the zeros of Φ as we vary ω for fixed y and λ; that is, we want to find the bifurcation diagrams of z versus ω. We asserted in the Introduction that qualitatively Φ has the bifurcation diagrams that are shown in Figure 1. To verify this point, we will use changes of coordinates in z, y, ω, λ of the form

$$\Psi(z, y, \omega, \lambda) = S(z, y, \omega, \lambda)\Phi(Z(z, y, \omega, \lambda), Y(y), \Omega(y, \omega, \lambda), \Lambda(\lambda))$$

to obtain a simpler function Ψ that is $\mathbf{S}^1$-equivalent to Φ. Remark 4.2 implies that the zeros of $\Psi(\cdot, y, \omega, \lambda)$ equal the zeros of $\Phi(\cdot, Y(y), \Omega(y, \omega, \lambda), \Lambda(\lambda))$. Thus, up to a change of coordinates in y and λ, the zeros of $\Psi(\cdot, y, \omega, \lambda)$ equal the zeros of $\Phi(\cdot, y, \Omega(y, \omega, \lambda), \lambda)$. For fixed y and λ, the function $\omega \mapsto \Omega(y, \omega, \lambda)$ is a change of coordinates in ω. Hence, the set of all bifurcation diagrams of z versus ω for fixed y and λ is the same qualitatively for the family $\Phi(z, y, \omega, \lambda)$ and the family $\Psi(z, y, \omega, \lambda)$. Then we compute the transition variety using singularity theory to find the bifurcation diagrams of Ψ.

We write η_1 and η_2 so that (4.4) has the form

$$\Phi(z, y, \eta) = (\eta_1 + i\eta_2 - |z|^2)z + y, \tag{5.1}$$

where

$$\eta_1 = c_1\lambda + d_1\omega + \mathcal{O}((\omega, \lambda)^2) \quad \text{and} \quad \eta_2 = c_2\lambda + d_2\omega + \mathcal{O}((\omega, \lambda)^2) \tag{5.2}$$

and $c_1, d_1, c_2, d_2 \in \mathbf{R}$. We assume that Φ is a universal unfolding (which should be true generically) and hence that $c_1d_2 - c_2d_1 \neq 0$ by the linear independence of η_ω and η_λ over $\mathbf{R}$ (see Proposition 4.6).

In the next proposition we simplify the form of Φ at linear order by changes of coordinates. We do this in such a way that the role of ω as a distinguished bifurcation parameter is preserved. More precisely, we assume that the coordinate changes in λ and y are independent

of ω. In this way we preserve the changes in multiplicity of solutions in the bifurcation diagrams formed by variation of ω.

Proposition 5.1. *Φ is equivalent, by a change of coordinates that preserves the bifurcation parameter ω, to*

$$\Psi(\tilde{z},\tilde{y},\tilde{\omega},\tilde{\lambda}) = (\tilde{\eta}_1(\tilde{\omega},\tilde{\lambda}) + i\tilde{\eta}_2(\tilde{\omega},\tilde{\lambda}) - (1+i\gamma)|\tilde{z}|^2)\tilde{z} + \tilde{y}, \tag{5.3}$$

where

$$\tilde{\eta}_1 = \tilde{\lambda} + \mathcal{O}((\tilde{\omega},\tilde{\lambda})^2) \quad \textit{and} \quad \tilde{\eta}_2 = \tilde{\omega} + \mathcal{O}((\tilde{\omega},\tilde{\lambda})^2). \tag{5.4}$$

Proof. To simplify the form of (5.1), we take the linear transformations

$$\begin{array}{lll} \Phi \to \alpha_1\Phi, & z \to \alpha_2\tilde{z}, & y \to \alpha_3\tilde{y}, \\ \omega \to A_1\tilde{\omega} + A_2\tilde{\lambda}, & & \lambda \to A_3\tilde{\lambda}, \end{array} \tag{5.5}$$

where $\alpha_1,\alpha_2,\alpha_3 \in \mathbf{C}$, $A_1,A_2,A_3 \in \mathbf{R}$, and $\alpha_1,\alpha_2,\alpha_4,A_1,A_3$ are nonzero. Then we have that

$$\begin{aligned} \Psi(\tilde{z},\tilde{y},\tilde{\omega},\tilde{\lambda}) &\equiv \alpha_1\Phi(\alpha_2\tilde{z},\alpha_3\tilde{y},A_1\tilde{\omega}+A_2\tilde{\lambda},A_3\tilde{\lambda}) \\ &= \alpha_1\alpha_2(((c_1+ic_2)A_3+(d_1+id_2)A_2)\tilde{\lambda} + (d_1+id_2)A_1\tilde{\omega} - |\alpha_2|^2|\tilde{z}|^2)\tilde{z} \\ &\quad + \alpha_1\alpha_3\tilde{y} + \mathcal{O}((\tilde{\omega},\tilde{\lambda})^2)\tilde{z}. \end{aligned} \tag{5.6}$$

Choose $\alpha_1\alpha_2$, A_2, A_3 satisfying

$$-\frac{A_2+iA_1}{A_3} = \frac{c_1+ic_2}{d_1+id_2}, \qquad \alpha_1\alpha_2 = \frac{1}{(d_2-id_1)A_1}$$

such that

$$\alpha_1\alpha_2((c_1+ic_2)A_3+(d_1+id_2)A_2) = 1 \quad \text{and} \quad \alpha_1\alpha_2((d_1+id_2)A_1) = i. \tag{5.7}$$

Note that this can be done since $c_1d_2 - c_2d_1 \neq 0$, i.e., $\frac{c_1+ic_2}{d_1+id_2} \notin \mathbf{R}$, by Proposition 4.6.

Pick up A_1 and α_2 such that A_1 has the same sign as d_2 and α_2 has the norm $\sqrt{\frac{A_1(d_1^2+d_2^2)}{d_2}}$. Then, the real part of the coefficient of $|z|^2z$ is -1, i.e.,

$$(\alpha_1\alpha_2)_R|\alpha_2|^2 = \frac{d_2|\alpha_2|^2}{A_1(d_1^2+d_2^2)} = 1 \tag{5.8}$$

by the second equation of (5.7).

By (5.7), (5.8) and choosing α_3 such that

$$\alpha_1\alpha_3 = 1,$$

we obtain that

$$\Psi(\tilde{z},\tilde{y},\tilde{\omega},\tilde{\lambda}) = (\tilde{\lambda} + i\tilde{\omega} - (1+i\gamma)|\tilde{z}|^2)\tilde{z} + \tilde{y} + \mathcal{O}((\tilde{\omega},\tilde{\lambda})^2)\tilde{z}, \tag{5.9}$$

where

$$\gamma = (\alpha_1\alpha_2)_I|\alpha_2|^2 = \frac{d_1|\alpha_2|^2}{A_1(d_1^2+d_2^2)} = \frac{d_1}{d_2}. \tag{5.10}$$

We can also write (5.9) in the form (5.3) for convenience. ∎

Remark 5.2. We trace through the calculation performed in section 3 for the normal form, and find that γ is exactly the ratio of the imaginary and real parts of the coefficient for the cubic term $|z|^2z$ in ψ. In fact, the form of Ψ in (5.3) is consistent with ψ. See Appendix C for the details.

For simplicity, we drop the tildes in the form of Ψ from now on; i.e.,

$$\Psi(z, y, \omega, \lambda) = (\eta_1(\omega, \lambda) + i\eta_2(\omega, \lambda) - (1 + i\gamma)|z|^2)z + y, \tag{5.11}$$

where

$$\eta_1 = \lambda + \mathcal{O}((\omega, \lambda)^2) \quad \text{and} \quad \eta_2 = \omega + \mathcal{O}((\omega, \lambda)^2). \tag{5.12}$$

We use singularity theory to analyze the bifurcation problem of the complex-valued function Ψ. To do this, we need to transform the problem to a problem of a real-valued function.

Lemma 5.3. *For fixed y and λ, Ψ has the same bifurcation diagrams as*

$$H(R; \omega, \lambda, \varepsilon) \equiv (1 + \gamma^2)R^3 - 2(\eta_1 + \gamma\eta_2)R^2 + (\eta_1^2 + \eta_2^2)R - \varepsilon^2, \tag{5.13}$$

where $R = |z|^2$, $\varepsilon = |y|$, and η_1 and η_2 are functions in ω and λ, as shown in (5.12).

Note that we have now derived the function H that was discussed in the Introduction. See (1.8).

Proof. Set $\Psi = 0$ and let $y = \varepsilon e^{i\theta}$. Then we have that

$$(\eta_1 + i\eta_2 - (1 + i\gamma)|v|^2)v = -\varepsilon e^{i\theta}. \tag{5.14}$$

Take the square of the norm of each side of (5.14) and let $R \equiv |z|^2$; then we obtain $H = 0$, where H is defined in (5.13). Thus, we are done. ∎

6. Transition set. In this section, we specify the transition variety associated with the bifurcation problem using singularity theory [10], by which we obtain Figure 1 eventually.

By [10], we define *the transition set* Σ of *hysteresis* $\mathcal{H}$, *bifurcation* $\mathcal{B}$, and *double limit points* $\mathcal{D}$ as

$$\Sigma = \mathcal{H} \cup \mathcal{B} \cup \mathcal{D},$$

where

$$\begin{aligned}
\mathcal{H} = \{\lambda, \varepsilon \in \mathbf{R} : \exists (R, \omega) \in \mathbf{R} \times \mathbf{R} \text{ such that } H = H_R = H_{RR} = 0,\\
H_{RRR} \neq 0 \text{ at } (R, \omega)\},\\
\mathcal{B} = \{\lambda, \varepsilon \in \mathbf{R} : \exists (R, \omega) \in \mathbf{R} \times \mathbf{R} \text{ such that } H = H_R = H_\omega = 0 \text{ at } (R, \omega)\},\\
\mathcal{D} = \{\lambda, \varepsilon \in \mathbf{R} : \exists (R_1, R_2, \omega) \in \mathbf{R} \times \mathbf{R} \times \mathbf{R}, R_1 \neq R_2 \text{ such that}\\
H = H_R = 0 \text{ at } (R_i, \omega), i = 1, 2\}.
\end{aligned}$$

The set $\mathcal{D}$ is empty, since the degree of H is 3 and the minimum degree for occurrence of double limit points is 4. For $\mathcal{H}$, we have the following claim.

Proposition 6.1. *Given nonzero γ, there exist curves of hysteresis points of H on the $\lambda\varepsilon$ plane, whose equations are*

$$\begin{aligned} \mathcal{H}_+ &: \ (3+\sqrt{3}\gamma)^3\varepsilon^2 = 8(1+\gamma^2)\eta_1^3, \\ \mathcal{H}_- &: \ (3-\sqrt{3}\gamma)^3\varepsilon^2 = 8(1+\gamma^2)\eta_1^3, \end{aligned} \tag{6.1}$$

where $\eta_1 = \lambda + \mathcal{O}((\varepsilon^{\frac{2}{3}}, \lambda)^2)$.

Proof. See Appendix D. ∎

Additionally, for $\mathcal{B}$, we have the following.

Proposition 6.2. *For any given $\gamma \neq 0$, H has a bifurcation point when (λ, ε) is on the curve*

$$\mathcal{B} : \ \varepsilon^2 = \frac{4}{27}\lambda^3 + \mathcal{O}(\lambda^4). \tag{6.2}$$

Proof. See Appendix D. ∎

Therefore, we have the transition set $\Sigma = \mathcal{H}_+ \cup \mathcal{H}_- \cup \mathcal{B}$, where the equations for $\mathcal{H}_+$, $\mathcal{H}_-$, and $\mathcal{B}$ are given in (6.1) and (6.2). As shown in Figure 1, the curves of Σ separate the parameter plane into four regions. More precisely, when $0 < \gamma < \sqrt{3}$, by (6.1) the hysteresis curves are

$$\varepsilon^{\frac{2}{3}} = \frac{2(1+\gamma^2)^{\frac{1}{3}}}{3 \pm \sqrt{3}\gamma}\lambda + \mathcal{O}((\lambda, \varepsilon^{\frac{2}{3}})^2).$$

So, solving for $\varepsilon^{\frac{2}{3}}$ gives

$$\varepsilon^{\frac{2}{3}} = \frac{2(1+\gamma^2)^{\frac{1}{3}}}{3 \pm \sqrt{3}\gamma}\lambda + \mathcal{O}(\lambda^2),$$

i.e.,

$$\varepsilon^2 = \frac{8(1+\gamma^2)}{(3 \pm \sqrt{3}\gamma)^3}\lambda^3 + \mathcal{O}(\lambda^4).$$

By Proposition 6.2, the bifurcation curve has the form

$$\varepsilon^2 = \frac{4}{27}\lambda^3 + \mathcal{O}(\lambda^4).$$

Since

$$0 < \frac{4}{27} < \frac{8(1+\gamma^2)}{(3+\sqrt{3}\gamma)^3} < \frac{8(1+\gamma^2)}{(3-\sqrt{3}\gamma)^3},$$

the two hysteresis curves are both on the right half of the $\lambda\varepsilon$ plane, and the bifurcation curve is even below the lower hysteresis curve.

When $\gamma > \sqrt{3}$, we have the following inequalities:

$$\frac{8(1+\gamma^2)}{(3-\sqrt{3}\gamma)^3} < 0 < \frac{8(1+\gamma^2)}{(3+\sqrt{3}\gamma)^3} < \frac{4}{27}.$$

So, one of the hysteresis curves is on the left half plane, the other on the right. Further, the bifurcation curve is a little higher than the hysteresis curve which is on the right half plane.

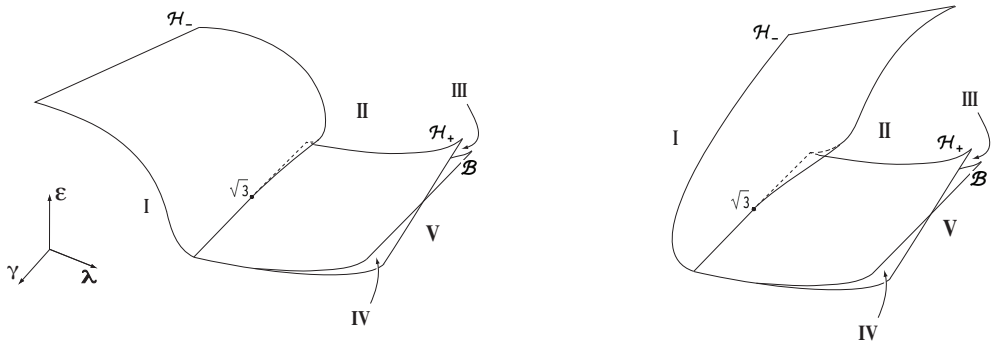

(a) $a_3 > 0$. (b) $a_3 < 0$.

Figure 10. (a) *and* (b) *are the graphs of the transition set* Σ *for* $a_3 > 0$ *and* $a_3 < 0$*, respectively, assuming that* η_1 *has the form* (6.3).

Recall that the bifurcation diagrams change only on the transition set Σ (see Theorem 6.1 of [10]). This means that in each of the four regions (excluding the boundaries) there is a unique type of bifurcation diagram. So, to figure out all possible bifurcation diagrams, we need only to pick up one point in each region and draw the bifurcation diagram occurring at this point. In this way, we obtain Figure 1.

Note that Figure 1 includes the bifurcation diagrams for two cases: $0 < \gamma < \sqrt{3}$ and $\gamma > \sqrt{3}$. But what happens near $\gamma = \sqrt{3}$? To understand the transition of bifurcation diagrams between Figures 1(a) and 1(b) as γ goes across $\sqrt{3}$, we sketch the graph of the transition set Σ in $(\lambda, \varepsilon, \gamma)$ space.

Assume that η_1 in (6.1) has the form

$$\eta_1 = \lambda + a_1\lambda^2 + a_2\lambda\varepsilon^{\frac{2}{3}} + a_3\varepsilon^{\frac{4}{3}} + \mathcal{O}((\lambda, \varepsilon^{\frac{2}{3}})^3), \tag{6.3}$$

where $a_1, a_2, a_3 \in \mathbf{R}$. As shown in Figure 10, depending on the sign of a_3, the $\mathcal{H}_-$ surface has two possible different shapes. However, the shapes do not actually affect the classification of bifurcation diagrams. More precisely, according to Figure 10, we find the following.

Proposition 6.3. *Suppose* $\gamma \sim \sqrt{3}$*. As* ω *varies, the bifurcation diagram of* H *is of*

(i) *type* I *when* $(\lambda, \varepsilon, \gamma)$ *is on the left of the surface* $\mathcal{H}_-$*;*
(ii) *type* II *when* $(\lambda, \varepsilon, \gamma)$ *is on the right of the surface of* $\mathcal{H}_-$ *and above* $\mathcal{H}_+$ *and* $\mathcal{B}$*;*
(iii) *type* III *when* $(\lambda, \varepsilon, \gamma)$ *is below* $\mathcal{H}_+$ *but above* $\mathcal{B}$*;*
(iv) *type* IV *when* $(\lambda, \varepsilon, \gamma)$ *is below* $\mathcal{B}$ *but above* $\mathcal{H}_+$*;*
(v) *type* V *when* $(\lambda, \varepsilon, \gamma)$ *is below* $\mathcal{H}_+$ *and* $\mathcal{B}$*,*

where equations for $\mathcal{H}_-$*,* $\mathcal{H}_+$*, and* $\mathcal{B}$ *are in* (6.1) *and* (6.2)*, and* η_1 *is in* (6.3).

Proof. See Appendix E. ∎

Appendix A. Conditions for occurrence of a Hopf bifurcation. Suppose that the ODE system (1.1) undergoes a generic Hopf bifurcation at $\lambda = 0$ when $G(t) = 0$. More precisely, together with (1.2), the following conditions are satisfied:

(a) as λ crosses 0, the imaginary eigenvalues of $A(\omega, \lambda)$ cross the imaginary axis at a

positive speed, i.e.,

$$\mathrm{Re}(\bar{d}^T A_\lambda(0)c) \neq 0,$$

where A_λ is the derivative of A with respect to λ, and c and d are nonzero vectors such that

$$A(0)c = ic, \qquad A(0)^t d = -id;$$

(b) the higher-order terms of F satisfy

$$\begin{aligned}&\mathrm{Re}\bar{d}^t A_\lambda(0)c \neq 0,\\ &\mathrm{Re}\{\bar{d}^t[d^2F(c,b_0) + d^2F(\bar{c},b_2) + \tfrac{1}{4}d^3F(c,c,\bar{c})]\} \neq 0,\end{aligned}$$

where the differentiation of F is with respect to x at the origin and b_0, b_2 satisfy

$$A(0)b_0 = \frac{1}{2}d^2F(c,\bar{c}), \qquad (A(0) - 2iI)b_2 = \frac{1}{4}d^2F(c,c).$$

Appendix B. Proof of Proposition 3.4. The proof of this proposition requires two lemmas. In the first we compute the generators for a general tangent space, and in the second the tangent space of bifurcations satisfying (3.6).

Lemma B.1. *For any $\zeta = pz + qy \in \vec{\mathcal{E}}_{z,y}(\mathbf{S}^1)$, $RT(\zeta, \mathbf{S}^1)$ has the 12 generators*

$$\begin{aligned}
S_1(z,y)\zeta &= [p^R, p^I, q^R, q^I],\\
S_2(z,y)\zeta &= [-p^I, p^R, -q^I, q^R],\\
S_3(z,y)\zeta &= [p^R v_1 + q^R v_3, -p^I v_1 - q^I v_3, -q^R v_1, q^I v_1],\\
S_4(z,y)\zeta &= [p^I v_1 + q^I v_3, p^R v_1 + q^R v_3, -q^I v_1, -q^R v_1],\\
S_5(z,y)\zeta &= [q^R v_2, -q^I v_2, p^R v_1, -p^I v_1],\\
S_6(z,y)\zeta &= [q^I v_2, q^R v_2, p^I v_1, p^R v_1],\\
S_7(z,y)\zeta &= [-p^R v_2, p^I v_2, q^R v_2 + p^R v_3, -q^I v_2 - p^I v_3],\\
S_8(z,y)\zeta &= [-p^I v_2, -p^R v_2, q^I v_2 + p^I v_3, q^R v_2 + p^R v_3],
\end{aligned} \tag{B.1}$$

and

$$\begin{aligned}
(d_z\zeta)z &= [p^R + 2p_1^R v_1 + p_3^R v_3, p^I + 2p_1^I v_1 + p_3^I v_3, 2q_1^R v_1 + q_3^R v_3, 2q_1^I v_1 + q_3^I v_3],\\
(d_z\zeta)(iz) &= [-p^I - 2q_3^I v_2 - p_3^I v_3, p^R + 2q_3^R v_2 + p_3^R v_3, 2p_3^I v_1 + q_3^I v_3, -2p_3^R v_1 - q_3^R v_3],\\
(d_z\zeta)y &= [2p_3^R v_2 + p_1^R v_3, 2p_3^I v_2 + p_1^I v_3, p^R + 2q_3^R v_2 + q_1^R v_3, p^I + 2q_3^I v_2 + q_1^I v_3],\\
(d_z\zeta)(iy) &= [2q_1^I v_2 + p_1^I v_3, -2q_1^R v_2 - p_1^R v_3, -p^I - 2p_1^I v_1 - q_1^I v_3, p^R + 2p_1^R v_1 + q_1^R v_3],
\end{aligned} \tag{B.2}$$

where $p_i = \frac{\partial p}{\partial v_i}(v_1, v_2, v_3)$, $p_i^R = \frac{\partial p^R}{\partial v_i}$ for $i = 1, 2, 3$, and similarly for q.

Proof. Because of the form for the restricted tangent space in (3.3), $RT(\zeta, \mathbf{S}^1)$ can be computed by the following two steps:

(a) Calculate $S\zeta$. Take any linear mapping $S(v, y)$. Suppose that

$$S(z,y)\zeta = \sum a_{jklm} z^j \bar{z}^k y^l \bar{y}^m \zeta + \sum b_{jklm} z^j \bar{z}^k y^l \bar{y}^m \bar{\zeta}. \tag{B.3}$$

Since S satisfies (3.2), i.e., $S(e^{i\theta}z, e^{i\theta}y)e^{i\theta}\zeta = e^{i\theta}S(z,y)\zeta$ for any $\theta \in \mathbf{S}^1$, we have that

$$\begin{aligned}
a_{jklm} &= 0 \qquad \text{if } j - k + l - m \neq 0,\\
b_{jklm} &= 0 \qquad \text{if } j - k + l - m \neq 2.
\end{aligned}$$

By the calculation in the proof of Lemma 2.2, we know that the generators of $S\zeta$ over $\vec{\mathcal{E}}_{z,y}(\mathbf{S}^1)$ are

$$S_1\zeta=\zeta, \quad S_2\zeta=i\zeta, \quad S_3\zeta=z^2\bar{\zeta}, \quad S_4\zeta=iz^2\bar{\zeta},$$
$$S_5\zeta=zy\bar{\zeta}, \quad S_6\zeta=izy\bar{\zeta}, \quad S_7\zeta=y^2\bar{\zeta}, \quad S_8\zeta=iy^2\bar{\zeta},$$

which yields (B.1).

(b) Calculate $(d_z\zeta)V$. Using

$$(d_z\zeta)u=\zeta_z u+\zeta_{\bar{z}}\bar{u}$$

and

$$\zeta_z=p_1v_1+p_3z\bar{y}+p+q_1\bar{z}y+q_3v_2, \quad \zeta_y=p_2z\bar{y}+p_3v_1+q_2v_2+q_3\bar{z}y+q,$$
$$\zeta_{\bar{z}}=p_1z^2+p_3zy+q_1zy+q_3y^2, \quad \zeta_{\bar{y}}=p_2zy+p_3z^2+q_2y^2+q_3zy,$$
$$z^2\bar{y}=v_3z-v_1y, \quad \bar{z}y^2=v_3y-v_2z,$$

we obtain the generators (B.2). ■

Lemma B.2. *Suppose that* $\zeta=pz+qy\in\vec{\mathcal{E}}_{z,y}(\mathbf{S}^1)$ *satisfies* (3.6). *Then*

$$\mathcal{N}\subset RT(\zeta,\mathbf{S}^1)+\mathcal{M}\mathcal{N}. \tag{B.4}$$

Proof. Modulo the submodule $\mathcal{M}\mathcal{N}$, the 12 generators for $RT(\zeta,\mathbf{S}^1)$ listed in (B.1) and (B.2) are shown in Table 2.

Table 2
The generators of $RT(\zeta,\mathbf{S}^1)$ *modulo* $\mathcal{M}\mathcal{N}$.

	v_1	v_2	v_3	v_1	v_2	v_3	1	1
$S_1(z,y)\zeta$	p_1^R	p_2^R	p_3^R	p_1^I	p_2^I	p_3^I	q^R	q^I
$S_2(z,y)\zeta$	$-p_1^I$	$-p_2^I$	$-p_3^I$	p_1^R	p_2^R	p_3^R	$-q^I$	q^R
$S_3(z,y)\zeta$			q^R			$-q^I$		
$S_4(z,y)\zeta$			q^I			q^R		
$S_5(z,y)\zeta$		q^R			$-q^I$			
$S_6(z,y)\zeta$		q^I			q^R			
$S_7(z,y)\zeta$								
$S_8(z,y)\zeta$								
$(d_z\zeta)z$	$3p_1^R$	p_2^R	$2p_3^R$	$3p_1^I$	p_2^I	p_3^I		
$(d_z\zeta)(iz)$	$-p_1^I$	$-p_2^I-2q_3^I$	$-2p_3^I$	p_1^R	$p_2^R+2q_3^R$	$2p_3^R$		
$(d_z\zeta)y$		$2p_3^R$	p_1^R		$2p_3^I$	p_1^I		
$(d_z\zeta)(iy)$		$2q_1^I$	p_1^I		$-2q_1^R$	p_1^R		

This matrix in the table has four blocks of columns: the elements in the first block are associated with $[*,0,0,0]$ and so on. Observe that $\{S_i(z,y)\zeta,\ i=3,4,5,6\}$ generate $\{[v_i,v_j,0,0]:i,j=2,3\}$ if $q(0)\neq 0$. Thus the 10×8 matrix is reduced to 6×4. This 6×4 matrix has rank 4 as long as $p_{v_1}(0)\neq 0$ and $q(0)\neq 0$. Hence, this whole matrix has rank 8, which implies that the generators of $\mathcal{N}$,

$$[v_i,0,0,0],[0,v_i,0,0],[0,0,1,0],[0,0,0,1], \quad i=1,2,3,$$

are contained in $RT(\zeta,\mathbf{S}^1)+\mathcal{M}\mathcal{N}$ and that (B.4) holds. ■

Proof of Proposition 3.4. The inclusion $\mathcal{N}\subset RT(\zeta,\mathbf{S}^1)$ follows from Nakayama's lemma [10] and (B.4). The reverse inclusion is verified by noting that

$$[c_1v_i,c_2v_j,c_3,c_4]\in\mathcal{N}$$

for $c_1, \dots, c_4 \in \mathbf{R}$ and $1 \le i, j \le 3$; i.e., each generator of $RT(\zeta, \mathbf{S}^1)$ is in $\mathcal{N}$. Thus, (3.8) is verified. ∎

Appendix C. Proof for Remark 5.2. Recall that ψ is the Liapunov–Schmidt reduction of the original system (1.5). By Proposition 2.8, we can assume that ψ has the form

$$\psi(z, y, \omega, \lambda) = ((-\sigma_\lambda(0) + i\kappa_\lambda(0))\lambda - i\omega + (a_1 + ib_1)v_1 + (a_2 + ib_2)v_2 + (a_3 + ib_3)v_3)z + (c + id)y + \text{h.o.t.}, \tag{C.1}$$

where $a_1, a_2, a_3, b_1, b_2, b_3, c, d \in \mathbf{R}$ and h.o.t. means the higher-order terms. We showed that $\Phi(z, y, \eta_1, \eta_2) = (\eta_1 + i\eta_2 - |z|^2)z + y$, where $\eta_1, \eta_2 \in \mathbf{R}$ is a universal unfolding of a normal form for $\psi(z, y, 0, 0)$, and Φ is equivalent to Ψ of (5.3). Recall that $-(1 + i\gamma)$ and $(a_1 + ib_1)$ are the coefficients of $|z|^2 z$ of Ψ and ψ, respectively. We will prove

$$\gamma = \frac{b_1}{a_1}. \tag{C.2}$$

We defined in (5.2) that $\eta_1 = c_1\lambda + d_1\omega$ and $\eta_2 = c_2\lambda + d_2\omega$. And we verified in (5.10) that $\gamma = \frac{d_1}{d_2}$. So, to show (C.2), it is sufficient to show

$$\frac{b_1}{a_1} = \frac{d_1}{d_2}. \tag{C.3}$$

Suppose that S and V are functions such that

$$\psi(z, y, \omega, \lambda) = S(z, y, \omega, \lambda)\Phi(V(z, y, \omega, \lambda), y, \omega, \lambda), \tag{C.4}$$

where V is $\mathbf{S}^1$-equivariant, $S(\theta z, \theta y, \omega, \lambda)\theta = S(z, y, \omega, \lambda)$ for any $\theta \in \mathbf{S}^1$, and $S(0) \neq 0$. At $y = \omega = \lambda = 0$,

$$\psi(z, 0, 0, 0) = S(z, 0, 0, 0)(-)|V(z, 0, 0, 0)|^2 V(z, 0, 0, 0). \tag{C.5}$$

However,

$$S(z, 0, 0, 0) = S(0, 0, 0, 0) + \mathcal{O}(|z|^2), \quad V(z, 0, 0, 0) = \alpha z + \mathcal{O}(|z|^2)z,$$

where $\alpha \in \mathbf{C}$ and

$$\psi(z, 0, 0, 0) = (a_1 + ib_1)|z|^2 z + \mathcal{O}(|z|^4)z$$

by (C.1). Thus, comparing the coefficients of $|z|^2 z$ on the left- and right-hand sides of (C.5) yields

$$a_1 + ib_1 = -S(0, 0, 0, 0)|\alpha|^2\alpha. \tag{C.6}$$

Similarly, we set $y = \lambda = 0$ and compare the coefficients of ωz of both sides of (C.5). It follows that

$$-i = S(0, 0, 0, 0)\alpha(d_1 + id_2).$$

Using (C.6) gives rise to

$$-i = -\frac{1}{|\alpha|^2}(a_1 + ib_1)(d_1 + id_2).$$

Thus,

$$a_1d_1 - b_1d_2 = \mathrm{Re}((d_1 + id_2)(a_1 + ib_1)) = 0.$$

This verifies (C.3).

Appendix D. Proof of Propositions 6.1 and 6.2. We use the following lemma to prove Proposition 6.1.

Lemma D.1. *For any $\varepsilon > 0$ and λ near 0, H has the hysteresis points (R_c, ω_c) when $\gamma = \gamma_c$, where*

$$R_c = \frac{\varepsilon^{\frac{2}{3}}}{(1+\gamma^2)^{\frac{1}{3}}}, \quad \eta_2^2 = 3\varepsilon^{\frac{4}{3}}(1+\gamma^2)^{\frac{1}{3}} - \eta_1^2, \quad \gamma\eta_2 = \frac{3}{2}\varepsilon^{\frac{2}{3}}(1+\gamma^2)^{\frac{2}{3}} - \eta_1 \tag{D.1}$$

and

$$\eta_1 = \lambda + \mathcal{O}((\omega_c, \lambda)^2), \quad \eta_2 = \omega_c + \mathcal{O}((\omega_c, \lambda)^2).$$

Proof. At the hysteresis point $(R, \omega) = (R_c, \omega_c)$, by [10], the following conditions are satisfied:

$$H = (1+\gamma^2)R^3 - 2(\eta_1 + \gamma\eta_2)R^2 + (\eta_1^2 + \eta_2^2)R - \varepsilon^2 = 0, \tag{D.2}$$

$$H_R = 3(1+\gamma^2)R^2 - 4(\eta_1 + \gamma\eta_2)R + (\eta_1^2 + \eta_2^2) = 0, \tag{D.3}$$

$$H_{RR} = 6(1+\gamma^2)R - 4(\eta_1 + \gamma\eta_2) = 0, \tag{D.4}$$

$$H_{RRR} = 6(1+\gamma^2) > 0.$$

By (D.4), it is clear that

$$R = \frac{2(\eta_1 + \gamma\eta_2)}{3(1+\gamma^2)}. \tag{D.5}$$

Plugging (D.5) into (D.3), we have

$$\eta_1^2 + \eta_2^2 = \frac{4(\eta_1 + \gamma\eta_2)^2}{3(1+\gamma^2)}. \tag{D.6}$$

Substituting (D.5) and (D.6) into (D.2) gives us

$$\eta_1 + \gamma\eta_2 = \frac{3}{2}\varepsilon^{\frac{2}{3}}(1+\gamma^2)^{\frac{2}{3}}. \tag{D.7}$$

Plugging (D.7) into (D.5) yields

$$R = \frac{\varepsilon^{\frac{2}{3}}}{(1+\gamma^2)^{\frac{1}{3}}}. \tag{D.8}$$

Meanwhile, applying (D.7) to (D.6) gives rise to

$$\eta_1^2 + \eta_2^2 = 3\varepsilon^{\frac{4}{3}}(1+\gamma^2)^{\frac{1}{3}}.$$

Therefore, (D.1) is verified. ∎

Let us now use Lemma D.1 to prove Proposition 6.1.

Proof of Proposition 6.1. By the last two equations of (D.1),

$$\gamma^2(3\varepsilon^{\frac{4}{3}}(1+\gamma^2)^{\frac{1}{3}}-\eta_1^2)=\left(\frac{3}{2}\varepsilon^{\frac{2}{3}}(1+\gamma^2)^{\frac{2}{3}}-\eta_1\right)^2,$$

i.e.,

$$(1+\gamma^2)^{\frac{2}{3}}\eta_1^2-3(1+\gamma^2)^{\frac{1}{3}}\varepsilon^{\frac{2}{3}}\eta_1+\frac{3}{4}(3-\gamma^2)\varepsilon^{\frac{4}{3}}=0. \tag{D.9}$$

Let

$$\tilde{\eta}=\frac{(1+\gamma^2)^{\frac{1}{3}}}{\varepsilon^{\frac{2}{3}}}\eta_1;$$

then (D.9) can be rewritten as

$$\tilde{\eta}^2-3\tilde{\eta}+\frac{9-3\gamma^2}{4}=0.$$

The solutions to this equation are

$$\tilde{\eta}=\frac{3\pm\sqrt{3}\gamma}{2},$$

i.e.,

$$\tilde{\eta}=\frac{(1+\gamma^2)^{\frac{1}{3}}}{\varepsilon^{\frac{2}{3}}}\eta_1=\frac{3\pm\sqrt{3}\gamma}{2}.$$

Therefore, we have the hysteresis curves

$$(3\pm\sqrt{3}\gamma)^3\varepsilon^2=8(1+\gamma^2)\eta_1^3, \tag{D.10}$$

where $\eta_1=\lambda+\mathcal{O}((\omega_c,\lambda)^2)$.

Since we want to draw the hysteresis curves on the $\lambda\varepsilon$ plane, we need (D.10) to depend only on λ and ε. For this purpose, we solve for ω_c as a function of λ and ε. By (D.5), we have that

$$Z(\omega,\lambda,R)\equiv\eta_1(\omega,\lambda)+\gamma\eta_2(\omega,\lambda)-\frac{3}{2}(1+\gamma^2)R=0 \tag{D.11}$$

at $(R,\omega)=(R_c,\omega_c)$. Since

$$Z_\omega=(\eta_1)_\omega+\gamma(\eta_2)_\omega=\gamma\neq 0,$$

there exists a unique function Ω such that

$$\omega_c=\Omega(\lambda,R_c)$$

by the implicit function theorem.

We can further find a more explicit expression of ω_c in terms of λ and ε. Substitute Ω into (D.11); then

$$\eta_1(\Omega(\lambda,R),\lambda)+\gamma\eta_2(\Omega(\lambda,R),\lambda)-\frac{3}{2}(1+\gamma^2)R=0$$

at $R=R_c$. Taking the derivative of this equation with respect to λ and R respectively, we have

$$\begin{aligned}&(\eta_1)_\omega\Omega_\lambda+(\eta_1)_\lambda+\gamma((\eta_2)_\omega\Omega_\lambda+(\eta_2)_\lambda)=0,\\&(\eta_1)_\omega\Omega_R+\gamma(\eta_2)_\omega\Omega_R-\tfrac{3}{2}(1+\gamma^2)=0.\end{aligned}$$

Thus, at $(\omega,\lambda)=(0,0)$,

$$\Omega_\lambda=-\frac{1}{\gamma},\qquad \Omega_R=\frac{3(1+\gamma^2)}{2\gamma}.$$

Therefore,

$$\omega=\Omega(\lambda,R)=-\frac{1}{\gamma}\lambda+\frac{3(1+\gamma^2)}{2\gamma}R+\mathcal{O}((\lambda,R)^2)$$

at $\omega=\omega_c$. Note that $\Omega(0,0)=0$ by (D.11) since $\eta_1(0,0)=\eta_2(0,0)=0$. By using (D.8), we can write

$$\omega_c=\tilde{\Omega}(\lambda,\varepsilon)=-\frac{1}{\gamma}\lambda+\frac{3(1+\gamma^2)^{\frac{2}{3}}}{2\gamma}\varepsilon^{\frac{2}{3}}+\mathcal{O}((\lambda,\varepsilon^{\frac{2}{3}})^2).$$

Thus, the hysteresis curves (D.10) can now be drawn in the $\lambda\varepsilon$ plane. ∎

Proof of Proposition 6.2. Assume that there is a point in $\mathcal{B}$. Then by the definition of $\mathcal{B}$, at this bifurcation point,

$$H=(1+\gamma^2)R^3-2(\eta_1+\gamma\eta_2)R^2+(\eta_1^2+\eta_2^2)R-\varepsilon^2=0, \tag{D.12}$$

$$H_R=3(1+\gamma^2)R^2-4(\eta_1+\gamma\eta_2)R+(\eta_1^2+\eta_2^2)=0, \tag{D.13}$$

$$H_\omega=-2((\eta_1)_\omega+\gamma(\eta_2)_\omega)R^2+2(\eta_1(\eta_1)_\omega+\eta_2(\eta_2)_\omega)R=0. \tag{D.14}$$

It follows from (D.14) that if $\gamma\neq 0$, then

$$\begin{aligned}R&=\frac{\omega+\mathcal{O}((\omega_c,\lambda)^2)}{\gamma+\mathcal{O}(\omega_c,\lambda)}\\&=\frac{1}{\gamma}(\omega+\mathcal{O}((\omega_c,\lambda)^2))(1+\mathcal{O}(\omega_c,\lambda))\\&=\frac{\omega}{\gamma}+\mathcal{O}((\omega_c,\lambda)^2).\end{aligned} \tag{D.15}$$

Applying (D.15) to (D.13), then

$$3R^2-4\lambda R+\lambda^2+\mathcal{O}((\omega_c,\lambda)^3)=0.$$

So,

$$R=\lambda+\mathcal{O}((\omega_c,\lambda)^2)\quad\text{ or }\quad R=\frac{\lambda}{3}+\mathcal{O}((\omega_c,\lambda)^2).$$

If $R = \lambda + \mathcal{O}((\omega_c, \lambda)^2)$, then by (D.15),

$$\omega_c = \gamma\lambda + \mathcal{O}((\omega_c, \lambda)^2).$$

So,

$$\varepsilon^2 = \mathcal{O}((\omega_c, \lambda)^4)$$

by using (D.12). Furthermore, since

$$H_{RR} = 2(1+\gamma^2)\lambda + \mathcal{O}((\omega_c, \lambda)^2) > 0$$

and

$$H_{\omega\omega} = \frac{2}{3}\lambda + \mathcal{O}((\omega_c, \lambda)^2) > 0,$$

there is an isola appearing in the system.

If $R = \frac{\lambda}{3} + \mathcal{O}((\omega_c, \lambda)^2)$, then by (D.15)

$$\omega = \frac{\gamma}{3}\lambda + \mathcal{O}((\omega_c, \lambda)^2)$$

at $\omega = \omega_c$. Solving this equation in (6.2) for ω_c, then

$$\omega_c = \frac{\gamma}{3}\lambda + \mathcal{O}(\lambda^2).$$

So, (D.12) gives rise to

$$\varepsilon^2 = \frac{4}{27}\lambda^3 + \mathcal{O}(\lambda^4). \tag{D.16}$$

Thus, we verify (6.2). ■

Appendix E. Proof of Proposition 6.3. When $\gamma = \sqrt{3}$, the hysteresis curves are

$$\mathcal{H}_+ : \ \varepsilon^2 = \frac{4}{27}\lambda^3 + \mathcal{O}(\lambda^4), \qquad \mathcal{H}_- : \ \eta_1 = \lambda + \mathcal{O}((\lambda, \varepsilon^{\frac{2}{3}})^2) = 0 \tag{E.1}$$

by Proposition 6.1, and the bifurcation curve

$$\mathcal{B} : \varepsilon^2 = \frac{4}{27}\lambda^3 + \mathcal{O}(\lambda^4) \tag{E.2}$$

by Proposition 6.2. From (E.1) and (E.2), we can see that when $\gamma \sim \sqrt{3}$, $\mathcal{H}_+$ is close to $\mathcal{B}$ and $\mathcal{H}_-$ to the ε-axis.

As shown in Figure 10, for fixed γ near $\sqrt{3}$, the curve of $\mathcal{H}_+$ may be below or above that of $\mathcal{B}$. But, in either case, by the calculation in Appendix D, Proposition 6.3(iii)–(v) are valid. We find that no new bifurcation diagram is generated by considering the higher-order terms of the equations for $\mathcal{H}_+$ and $\mathcal{B}$, compared to Figure 1.

Note that $\mathcal{H}_-$ is tangent to the λ-axis when $\gamma \neq \sqrt{3}$, but to the ε-axis when $\gamma = \sqrt{3}$. To understand this abrupt change of tangency as γ goes across the critical number $\sqrt{3}$, we use Figure 11 as an illustration. Suppose that

$$\eta_1 = \lambda + a_1\lambda^2 + a_2\lambda\varepsilon^{\frac{2}{3}} + a_3\varepsilon^{\frac{4}{3}} + \mathcal{O}((\lambda, \varepsilon^{\frac{2}{3}})^3), \tag{E.3}$$

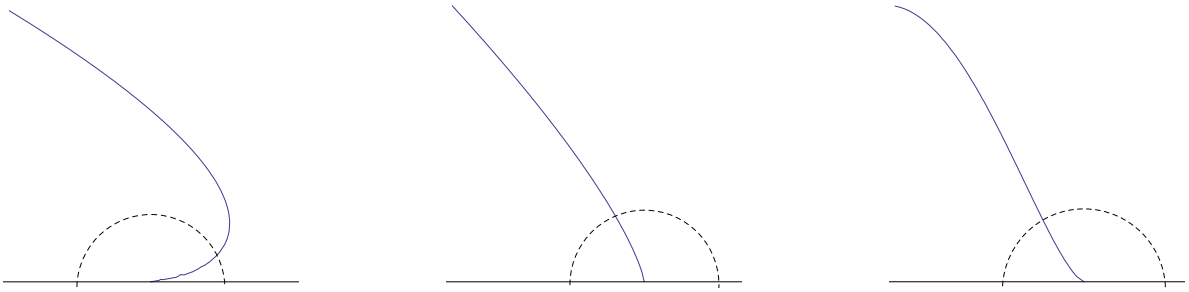

(a) $\gamma < \sqrt{3}$. (b) $\gamma = \sqrt{3}$. (c) $\gamma > \sqrt{3}$.

Figure 11. *The graphs of $\mathcal{H}_-$ as γ varies near $\sqrt{3}$, assuming that $\eta_1 = \lambda + a_1\lambda^2 + a_2\lambda\varepsilon^{\frac{2}{3}} + a_3\varepsilon^{\frac{4}{3}} + \mathcal{O}((\lambda, \varepsilon^{\frac{2}{3}})^3)$, where $a_i \in \mathbf{R}$, $i = 1, 2, 3$, and $a_3 > 0$.*

where $a_i \in \mathbf{R}$, $i = 1, 2, 3$, and $a_3 > 0$. Figure 11 shows that in a small neighborhood of the origin, the tangency of $\mathcal{H}_-$ changes as γ goes across $\sqrt{3}$ smoothly.

In fact, in a neighborhood of the origin, there are only two types of pictures of $\mathcal{H}_-$. By (6.1) and (E.3), we obtain

$$a_3\varepsilon^{\frac{4}{3}} - \left(\frac{3-\sqrt{3}\gamma}{2(1+\gamma^2)^{\frac{1}{3}}} - a_2\lambda\right)\varepsilon^{\frac{2}{3}} + \lambda + a_1\lambda^2 = \mathcal{O}((\lambda, \varepsilon^{\frac{2}{3}})^3). \tag{E.4}$$

In a small enough neighborhood, to sketch the picture of (E.4), it suffices to consider

$$a_3\varepsilon^{\frac{4}{3}} - \frac{3-\sqrt{3}\gamma}{2(1+\gamma^2)^{\frac{1}{3}}}\varepsilon^{\frac{2}{3}} + \lambda = 0. \tag{E.5}$$

Let

$$\mathcal{F}(\varepsilon^{\frac{2}{3}}, \lambda) = a_3\varepsilon^{\frac{4}{3}} - \frac{3-\sqrt{3}\gamma}{2(1+\gamma^2)^{\frac{1}{3}}}\varepsilon^{\frac{2}{3}} + \lambda.$$

Assume that $a_3 > 0$. For fixed λ, $\mathcal{F}$ has at most two zeros. And, for negative λ, $\mathcal{F}$ has a unique zero since $\mathcal{F}(0, \lambda) < 0$ and zeros of $\mathcal{F}$ are positive. Moreover,

$$\mathcal{F}(\varepsilon^{\frac{2}{3}}, 0) = \varepsilon^{\frac{2}{3}}\left(a_3\varepsilon^{\frac{2}{3}} - \frac{3-\sqrt{3}\gamma}{2(1+\gamma^2)^{\frac{1}{3}}}\right)$$

has two zeros if and only if $\gamma < \sqrt{3}$. So, we verify Figure 11. The case for $a_3 < 0$ can be analyzed similarly. ■

Appendix F. Proof of Theorem 1.2. To prove Theorem 1.2, we look at the Jacobian matrix of Ψ, where Ψ is defined in (1.10). We let

$$\Psi = \Psi_R + i\Psi_I, \qquad z = z_R + iz_I,$$

where $\Psi_R, \Psi_I, z_R, z_I \in \mathbf{R}$, and rewrite (1.10) as

$$\begin{aligned} \Psi_R &= (\lambda - |z|^2)z_R - (\omega - \gamma|z|^2)z_I + y_R = 0, \\ \Psi_I &= (\omega - \gamma|z|^2)z_R + (\lambda - |z|^2)z_I + y_I = 0. \end{aligned} \tag{F.1}$$

The Jacobian matrix of (F.1) is

$$D\Psi = \begin{bmatrix} \lambda - |z|^2 - 2z_R^2 + 2\gamma z_R z_I & -\omega + \gamma|z|^2 + 2\gamma z_I^2 - 2z_R z_I \\ \omega - \gamma|z|^2 - 2\gamma z_R^2 - 2z_R z_I & \lambda - |z|^2 - 2z_I^2 - 2\gamma z_R z_I \end{bmatrix}.$$

Let Λ be an eigenvalue of $D\Psi$. Then direct calculation leads to

$$\Lambda^2 - 2(\lambda - 2R)\Lambda + H_R = 0, \tag{F.2}$$

where $R = |z|^2$, the function H is defined in (5.13), and H_R is the derivative of H with respect to R. An equilibrium of Ψ is a

$$\begin{array}{ll} \text{sink} & \text{if } H_R > 0 \text{ and } \lambda - 2R < 0, \\ \text{source} & \text{if } H_R > 0 \text{ and } \lambda - 2R > 0, \\ \text{saddle} & \text{if } H_R < 0. \end{array} \tag{F.3}$$

Thus, to prove Theorem 1.2, it suffices to know the signs of H_R and $\lambda - 2R$. Note that changes in stability can occur only at saddle-node ($H_R = 0$) and Hopf ($\lambda = 2R$ and $H_R > 0$) bifurcations. Hopf bifurcations can be created locally in the bifurcation diagrams only at $\mathcal{TB}$ points in parameter space. (They can also be created globally by a point of Hopf bifurcation coming in from "∞." These global changes happen in the transitions between regions I(a) and I(b) and between II(a) and II(b) in Figure 9.) We discuss saddle-nodes, the eigenvalue crossing condition at Hopf bifurcations, and then the $\mathcal{TB}$-variety, before completing the proof of Theorem 1.2.

F.1. Saddle-node bifurcations. The sign of H_R changes at fold points ($H = H_R = 0$) of the bifurcation curve of R versus ω. Furthermore, $H_R < 0$ holds at (R_0, ω_0) if and only if there exist three different zeros of H at ω_0 and R_0 is the intermediate value of the three zeros.

F.2. Eigenvalue crossing condition. At a Hopf bifurcation point, $H = 0$, $R = \frac{\lambda}{2}$, and $H_R > 0$. Generic Hopf bifurcations satisfy two additional assumptions: the eigenvalue crossing condition (which guarantees the existence of a unique branch of periodic trajectories) and a third-order condition (which determines whether the branch is supercritical or subcritical and whether the periodic solutions on that branch are stable or not). The computation of the third-order condition (in the normal form at the point of Hopf bifurcation) will require terms of order higher than 3 in the truncated system (1.10), and its computation is beyond the scope of this paper. In this appendix we show that the eigenvalue crossing condition is always valid.

In the Introduction we noted that the eigenvalue crossing condition is equivalent to showing that $R_\omega \neq 0$ (see (1.11)). We now calculate R_ω at Hopf bifurcation point (ω, R) for fixed λ and ε. Recall that

$$H = (1+\gamma^2)R^3 - 2(\lambda + \gamma\omega)R^2 + (\lambda^2 + \omega^2)R - \varepsilon^2 = 0.$$

Taking the derivative with respect to ω, we then have

$$H_\omega = 3(1+\gamma^2)R^2 R_\omega - 4(\lambda + \gamma\omega)RR_\omega - 2\gamma R^2 + (\lambda^2 + \omega^2)R_\omega + 2\omega R = 0,$$

that is,

$$\left(3(1+\gamma^2)R^2 - 4(\lambda + \gamma\omega)R + \lambda^2 + \omega^2\right) R_\omega = 2\gamma R^2 - 2\omega R.$$

At $R = \frac{\lambda}{2}$,

$$\left(-\frac{\lambda^2}{4} + \frac{3}{4}\gamma^2\lambda^2 - 2\gamma\lambda\omega + \omega^2\right) R_\omega = \frac{\gamma}{2}\lambda^2 - \lambda\omega. \tag{F.4}$$

It follows that $R_\omega = 0$ if either $\lambda = 0$ or $\omega = \frac{\gamma\lambda}{2}$.

We substitute $R = \frac{\lambda}{2}$ into $H = 0$ to obtain

$$4\lambda\omega^2 - 4\gamma\lambda^2\omega + (1+\gamma^2)\lambda^3 - 8\varepsilon^2 = 0. \tag{F.5}$$

Note that if $\lambda = 0$, then $\varepsilon = 0$. But we can assume that $(\lambda, \varepsilon) \neq (0, 0)$. Hence we can assume $\omega = \frac{\gamma\lambda}{2}$ and substitute into (F.5), obtaining the cusp

$$\lambda^3 = 8\varepsilon^2.$$

Observe that along this cusp

$$H_R = 3(1+\gamma^2)R^2 - 4(\lambda + \gamma\omega)R + (\lambda^2 + \omega^2) = -\frac{1}{2}\lambda^2(3\gamma^2 + 1) < 0.$$

So zeros of R_ω do not occur at points of Hopf bifurcation. It follows that the Hopf bifurcation points lead to unique branches of periodic solutions in (1.10).

F.3. $\mathcal{TB}$-variety. The parameter values on the $\mathcal{TB}$-variety discussed in the Introduction are found by solving $H = H_R = \lambda - 2R = 0$; see (1.12). We begin by substituting $R = \frac{\lambda}{2}$ into

$$\begin{aligned} H &= (1+\gamma^2)R^3 - 2(\lambda + \gamma\omega)R^2 + (\lambda^2 + \omega^2)R - \varepsilon^2 = 0, \\ H_R &= \quad 3(1+\gamma^2)R^2 - 4(\lambda + \gamma\omega)R + (\lambda^2 + \omega^2) \quad = 0, \end{aligned}$$

obtaining

$$\begin{aligned} &\text{(a)} \quad (1+\gamma^2)\lambda^3 - 4\gamma\omega\lambda^2 + 4\omega^2\lambda = 8\varepsilon^2, \\ &\text{(b)} \quad (3\gamma^2 - 1)\lambda^2 - 8\gamma\omega\lambda + 4\omega^2 = 0. \end{aligned} \tag{F.6}$$

We can solve for ω by subtracting λ times (F.6)(b) from (F.6)(a), obtaining

$$(1-\gamma^2)\lambda^3 + 2\gamma\omega\lambda^2 = 4\varepsilon^2,$$

which is linear in ω. Thus

$$\omega = \frac{4\varepsilon^2 + (\gamma^2 - 1)\lambda^3}{2\gamma\lambda^2}. \tag{F.7}$$

To determine the $\mathcal{TB}$-variety we can substitute (F.7) into (F.6)(b) to obtain a curve in the $\lambda\varepsilon$ parameter plane where $\mathcal{TB}$ points occur. Specifically, we obtain

$$(\gamma^2 + 1)\lambda^6 - 8\varepsilon^2(\gamma^2 + 1)\lambda^3 + 16\varepsilon^4 = 0.$$

It follows that

$$\lambda^3 = 4\varepsilon^2\left(1 \pm \frac{\gamma}{\sqrt{\gamma^2 + 1}}\right); \tag{F.8}$$

that is, the $\mathcal{TB}$-variety consists of two cusps, and both cusps occur in the $\lambda > 0$ half plane.

F.4. Proof of Theorem 1.2. We have shown that the transitions between bifurcation diagrams as parameters λ and ε are varied are given by five cusp-like transition varieties: Bifurcation ($\mathcal{B}$), hysteresis ($\mathcal{H}_+$ and $\mathcal{H}_-$), and Takens–Bogdanov ($\mathcal{TB}_+$ and $\mathcal{TB}_-$). To lowest order these varieties are defined by

$$\mathcal{B}: \quad \lambda^3 = \frac{27}{4}\varepsilon^2, \tag{E.2}$$

$$\mathcal{H}_+: \quad \lambda^3 = \frac{(3+\sqrt{3}\gamma)^3}{8(1+\gamma^2)}\varepsilon^2, \tag{D.10}$$

$$\mathcal{H}_-: \quad \lambda^3 = \frac{(3-\sqrt{3}\gamma)^3}{8(1+\gamma^2)}\varepsilon^2, \tag{D.10}$$

$$\mathcal{TB}_+: \quad \lambda^3 = 4\left(1+\frac{\gamma}{\sqrt{\gamma^2+1}}\right)\varepsilon^2, \tag{F.8}$$

$$\mathcal{TB}_-: \quad \lambda^3 = 4\left(1-\frac{\gamma}{\sqrt{\gamma^2+1}}\right)\varepsilon^2. \tag{F.8}$$

For certain critical values of γ the cusp curves overlie each other and signify differences in the possible bifurcation diagrams in the ωR plane. For example, when $\gamma = \sqrt{3}$, $\mathcal{B}$ and $\mathcal{H}_+$ are identical to lowest order. All of the overlays are indicated in (F.9):

(F.9)

	$\mathcal{H}_+$	$\mathcal{TB}_+$	$\mathcal{TB}_-$
$\mathcal{B}$	$C_0 = \sqrt{3} \approx 1.73$	$C_3 = \frac{11}{3\sqrt{15}} \approx 0.95$	
$\mathcal{H}_+$		$C_4 \approx 5.66$	$C_1 \approx 0.06$
$\mathcal{H}_+$		$C_2^* = \frac{1}{\sqrt{3}} \approx 0.58$	

There are two overlays of $\mathcal{H}_+$ with $\mathcal{TB}_+$ at C_2 and C_4. The overlay at C_2 is not relevant since the varieties never cross (at lowest order), and we indicate this point by an asterisk. So there are four transition points in γ ($0 < C_1 < C_3 < C_0 < C_4 < \infty$) and five different regions of possible bifurcation diagrams. These regions are shown in Figure 9.

Acknowledgments. We thank Don Aronson, Edgar Knobloch, Claire Postlethwaite, and LieJune Shiau for helpful conversations.

REFERENCES

[1] A. K. Bajaj, *Resonant parametric perturbations of the Hopf bifurcation*, J. Math. Anal. Appl., 115 (1986), pp. 214–224.

[2] N. N. Bogoliubov and Y. A. Mitropolsky, *Asymptotic Methods in the Theory of Non-Linear Oscillations*, Hindustan Publishing Corporation, Delhi, India, 1961.

[3] J. Damon, *The unfolding and determinacy theorems for subgroups of $\mathcal{A}$ and $\mathcal{K}$*, Mem. Amer. Math. Soc., 50 (1984), no. 306.

[4] V. M. Eguíluz, M. Ospeck, Y. Choe, A. J. Hedspeth, and M. O. Magnasco, *Essential nonlinearities in hearing*, Phys. Rev. Lett., 84 (2000), pp. 5232–5235.

[5] C. Elphick, G. Iooss, and E. Tirapegui, *Normal form reduction for time-periodically driven differential equations*, Phys. Lett. A, 120 (1987), pp. 459–463.

[6] J. Furter, A. M. Sitta, and I. Stewart, *Singularity theory and equivariant bifurcation problems with parameter symmetry*, Math. Proc. Cambridge Philos. Soc., 120 (1996), pp. 547–578.

[7] J. M. Gambaudo, *Perturbation of a Hopf bifurcation by an external time-periodic forcing*, J. Differential Equations, 57 (1985), pp. 172–199.
[8] P. Glendinning and M. Proctor, *Travelling waves with spatially resonant forcing: Bifurcations of a modified Landau equation*, Internat. J. Bifur. Chaos Appl. Sci. Engrg., 3 (1993), pp. 1447–1455.
[9] M. Golubitsky, C. Postlethwaite, L.-J. Shiau, and Y. Zhang, *The feed-forward chain as a filter amplifier motif*, in Coherent Behavior in Neuronal Networks, Springer Ser. Comput. Neurosci. 3, K. Josic, M. Matias, R. Romo, and J. Rubin, eds., Springer-Verlag, New York, 2009, pp. 95–120.
[10] M. Golubitsky and D. Schaeffer, *Singularities and Groups in Bifurcation Theory* I, Appl. Math. Sci. 51, Springer-Verlag, New York, 1985.
[11] M. Golubitsky, I. Stewart, and D. Schaeffer, *Singularities and Groups in Bifurcation Theory* II, Appl. Math. Sci. 69, Springer-Verlag, New York, 1988.
[12] P. Gross, *On harmonic resonance in forced nonlinear oscillators exhibiting a Hopf bifurcation*, IMA J. Appl. Math., 50 (1993), pp. 1–12.
[13] G. Iooss, *Bifurcation of Maps and Application*, Math. Stud. 36, North–Holland, Amsterdam, 1979.
[14] W. L. Kath, *Resonance in a periodically perturbed Hopf bifurcation*, Stud. Appl. Math., 65 (1981), pp. 95–112.
[15] K. A. Montgomery, M. Silber, and S. A. Solla, *Amplification in the auditory periphery: The effect of coupling tuning mechanisms*, Phys. Rev. E, 75 (2007), 051924.
[16] N. S. Namachchivaya and S. T. Ariaratnam, *Periodically perturbed Hopf bifurcation*, SIAM J. Appl. Math., 47 (1987), pp. 15–39.
[17] S. Rosenblat and D. S. Cohen, *Periodically perturbed bifurcation*-II *Hopf bifurcation*, Stud. Appl. Math., 64 (1981), pp. 143–175.
[18] Y. Zhang, *Periodic Forcing of a System Near a Hopf Bifurcation Point*, Ph.D. thesis, Department of Mathematics, The Ohio State University, Columbus, OH, 2010.